MODIFICATION OF NITRIC OXIDE (NO) RELEASING POLYMERS FOR ENHANCED BROAD-SPECTRUM ANTIMICROBIAL ACTIVITY

by

CHRISTINA DANIELLE WORKMAN

(Under the Direction of Hitesh Handa)

ABSTRACT

Indwelling medical devices have provided significant enhancement to patient's outcomes, but often come with the risk of infection. Increasing numbers of antibiotic-resistant bacteria have prompted researchers to discover innovative methods to treat and prevent these infections. Nitric oxide (NO) is a free radical produced by endothelial cells, macrophages, and neurons that has demonstrated excellent antimicrobial properties. The incorporation of NO donors within medical grade polymers to mimic endogenous NO release has shown the potential to reduce infection rates and subsequent antibiotic use. Before these materials can move to clinical use some improvements are necessary. Herein, two novel methods of enhancing NO release are described: 1) the addition of a metal ion to catalyze NO release from a S-nitrosothiol donor and 2) covalent attachment of the NO donor directly to the polymer. These modifications allowed for prolonged duration of NO release, increased NO levels, and improved antimicrobial activity.

INDEX WORDS: Nitric Oxide, Antimicrobial, Nanoparticles, Polyurethane

MODIFICATION OF NITRIC OXIDE (NO) RELEASING POLYMERS FOR ENHANCED BROAD-SPECTRUM ANTIMICROBIAL ACTIVITY

by

CHRISTINA DANIELLE WORKMAN

BSA, University of Georgia, 2016

A Thesis Submitted to the Graduate Faculty of The University of Georgia in Partial Fulfillment of the Requirements for the Degree

MASTER OF SCIENCE

ATHENS, GEORGIA

2018

MODIFICATION OF NITRIC OXIDE (NO) RELEASING POLYMERS FOR ENHANCED BROAD-SPECTRUM ANTIMICROBIAL ACTIVITY

by

CHRISTINA DANIELLE WORKMAN

Major Professor: Hitesh Handa

Committee: James Warnock
William Kisaalita

Electronic Version Approved:

Suzanne Barbour
Dean of the Graduate School
The University of Georgia
December 2018

ACKNOWLEDGEMENTS

First, I would like to extend my sincerest gratitude to my major professor, Dr. Hitesh Handa. Thank you for having confidence in me and allowing me to continue my research in your biomaterials lab. Without your help, I would not be on my way to physician assistant school this May.

Secondly, I owe a huge thanks to my lab members for teaching me and supporting me. Specifically, I have to thank Katie Homeyer, a reliable study partner and group project aficionado. Priya Singha, thank you for being my mentor from the beginning of my research journey. Dr. Sean Hopkins, thank you for answering all of my questions and providing everyone with the coffee fuel to make it through a master's degree.

Last, but certainly not least, I have to thank my family and friends. Mom, thanks for sticking with me through it all, even on my bad days. I owe you big time. Thank you to all my friends that listened to me talk about things that probably did not interest them. I am grateful to have such a wonderful support team.

TABLE OF CONTENTS

Page

LIST OF TABLES

Page

LIST OF FIGURES

Page

CHAPTER 1

INTRODUCTION

1.1 Hospital-Acquired Infections

Indwelling medical devices have allowed for rapid growth in the practice of medicine and have contributed greatly to the quality of life. While these devices are indispensable for the treatment and prevention of many diseases and complications, they are often associated with an increased risk of Infection. Healthcare-associated infections (HAIs) are defined by their absence at time of admission, but acquired during a patient's hospitalization. HAIs impact an estimated 1 in 25 patients in acute care hospital settings with an observed mortality rate of 100,000 deaths per year in the United States (US) alone.[1,2] HAIs are generally broken into 4 types: blood stream infections, surgical site infections, urinary tract infections, and device-related infections. Together, the morbidity of these HAIs contributes to roughly $20 billion spent annually as reported by the Centers for Disease Control and Prevention (CDC).[3] These statistics cause growing alarm, as the scope of medical device technology continues to expand.

Common device-related HAIs of significant concern include ventilator-associated pneumonia (VAP), catheter-related bloodstream infections (CRBSI), and catheter-associated urinary tract infections (CAUTI). Out of the 3 million central venous catheters inserted each year in the US, 28% of the resulting infected catheters will lead to mortality.[4] Compared to other types of HAIs, VAPs are associated with the highest rate

of mortality, ranging from 24-50%.[5] Risk factors for the development of the aforementioned infections are location of the device, duration of use, and host factors (age, preexisting conditions, etc.). The use of these devices that lead to infection is consistently increasing due to the rise in hospitalization rates, along with a large aging population. This makes reducing the spread of infection and surveillance of device-related infections a high priority for all healthcare providers. Proper precautions for reducing the spread of infection, such as hand washing, should also be maintained.

1.2 Pathogenesis of Implantable Device Infections

An infection is acquired when there is an imbalance in the host tissue and foreign microorganisms. The pathogens that are often associated with nosocomial infections are considered either gram-negative or gram-positive bacteria, denoting the presence and structure of the outer membrane. Common cultured organisms from HAIs include gram-negative *Escherichia coli (E. coli), Pseudomonas aeruginosa (P. aeruginosa),* and *Proteus mirabilis*, and the infamous gram-positive bacteria, *Staphylococcus aureus (S. aureus),* known as the leading cause of infections in indwelling medical devices.[6] Most of these bacteria can be found on the skin, in water, or on improperly cleaned surfaces and equipment. Although these bacteria normally reside in these areas with little notice, they quickly become virulent when given an opportunity, such as a host's weakened immune system or an exposed wound on the skin. In a clinical setting, transmission of bacterial organisms can happen through direct contact with bodily fluids or through air particles. Transmission can easily happen from a patient's contact with an infected patient or passed from a healthcare worker that was in contact with an infected patient.

Upon implantation of a medical device within a biological environment, such as a venous catheter in the bloodstream, a series of events take place that lead to its colonization with bacteria. Initially, planktonic bacteria form weak interactions with the device surface, mainly through reversible Van der Waals forces.[7] These once free-floating bacteria cells now attract more cells to the device surface and begin secreting an extracellular polymeric substances (EPS) designed to hold the cells together. The secreted matrix also supports stronger adhesion to the surface and provides a protective barrier from antimicrobial penetration and macrophage engulfment. Maturation of the biofilm is then dependent on cell-to-cell communication through signaling molecules and a phenomenon known as quorum sensing. Quorum sensing allows the bacteria to work as a single unit and react to the environment surrounding them.[8] As the bacteria continue to develop and colonize the surface, some cells may detach and disperse into the biological environment leading to the spread of infection within the host. The complete lifecycle of a biofilm on a medical device surface is depicted in Figure 1.1.

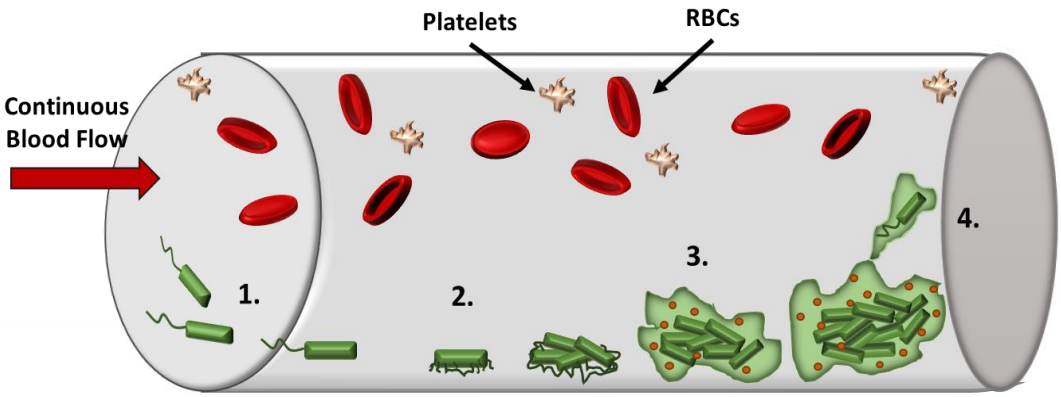

Figure 1.1. Biofilm formation on a material surface goes through 4 distinct phases: 1) Initial presence and transport of planktonic bacteria 2) Irreversible attachment to surface and excretion of EPS 3) Biofilm maturation 4) Bacteria detachment and dispersal

Biofilm contamination and the resultant bacterial dissemination contributes to the device failure and the development of complications, such as ventilator-associated pneumonia, catheter-associated urinary tract infections, and surgical-site infections.[9] Removal and replacement of the infected device is the typical clinical approach, followed by a course of antibiotics for bloodstream infections. Penicillin was the first antibiotic available to doctors in the early 1940's, beginning the golden era of antibiotics.[10] Over the years the improper prescribing and extensive use of antibiotics has resulted in the prevalence of bacterial resistance. More than 15 classes of antibiotic drugs have been implicated in the escalating frequency of resistant bacteria strains.[11,12] *Staphylococcus aureus* has shown multi-drug resistance, beginning with the emergence of methicillin-resistant *S. aureus* (MRSA) discovered nearly 50 years ago.[13] In 2002, 57% of *S. aureus* isolated presented as MRSA.[14] The spread of MRSA prompted the introduction of vancomycin as the standard treatment for *S. aureus* infections, but resistance has been

quickly established leading to vancomycin-resistant *S. aureus* (VRSA). While the occurrence of VRSA is rare when compared to MRSA, it continues to provide apprehension about the future outlook of antibiotic use. Moreover, bacteria residing within a biofilm are over 1,000 times more resistant to antibiotics.[15]

The growing alarm of antibiotic resistance has provoked changes in the methodology that medical providers use to prescribe and administer antibiotics. Many facilities now require positive identification of the infecting organism prior to a decision of medical care. From a pharmaceutical standpoint, there have been a reduction in companies that invest in antibiotic development due to high risk and an estimated inevitability of bacterial resistance within 2 years of use.[16] The diminishing role of antibiotics is a motivating factor for scientist and researchers to continually pursue new avenues for treatment and prevention of bacterial infections.

1.3 Biocompatibility of Medical Devices

Almost all implantable devices are faced with the challenge of the body's foreign body response (FBR), initiated upon integration of a foreign material. The FBR is characterized by events such as initiation of macrophages and blood protein deposition on the material's surface. In order to avoid a strong FBR, materials can be designed to be biocompatible. The biocompatibility of a medical devices is defined by its degree of interaction with the host tissue and the ability of the device to co-exist within the host without eliciting harmful local or systemic effects.[17,18] When a material lacks biocompatibility the host may respond in a variety of ways, including deposition of protein on the material surface, activation of immune system, or initiation of thrombus formation.[18,19] Materials recognized as foreign cause the body to react harshly, creating

more serious complications. For example, a foreign material that causes thrombus formation on its surface has the possibility of the formed thrombi to block blood flow, as well as detach and cause an embolism elsewhere in the body. In this case, the material causes additional harm to the patient and could lead to a fatal outcome. A full assessment of biocompatibility of a developed device is typically achieved through *in vitro* studies that look at fibroblast cell viability after exposure to the material and its leachates.

The determination of a material's biocompatibility can also predict the potential interaction of bacteria. Material surfaces that are prone to protein deposition facilitate bacteria adhesion.[20] The process of bacterial adhesion is also influenced by the characteristics of the individual bacteria and the surrounding medium.[21] Since we cannot change the nature of the bacteria or the medium encountered in medical applications, the surface of the implant is the only area where significant modification can occur. Surface characteristics can be adjusted without impacting the bulk properties of the material through the use of coatings and chemical functionalization.[22] Specific methods for material modification will be further discussed in section 1.4. When designing materials, it is important to consider the medium that the material will contact. Properties of the medium that have a role in bacteria adhesion involve shear stress of the medium flow, concentration of bacteria, temperature, and surface tension of the medium.[21,23,24] For indwelling medical devices, mediums that are typically encountered are blood and urine.

Characteristics of bacteria that impact their ability to adhere include the presence of protein-based structures, such as pili and flagella, surface charge, and bacterial hydrophobicity. Bacteria in aqueous solutions frequently carry a negative surface charge, which may enhance attachment to medical devices depending on the surface

functionalization of the material.[25] Another important physical factor for bacterial adhesion is the bacteria's hydrophobicity. Hydrophobic bacteria tend to have a stronger affinity for adherence to hydrophobic material surfaces and hydrophilic bacteria tend to have a stronger affinity for more hydrophilic material surfaces.[26] There is a greater extent of bacterial adhesion in hydrophobic interactions, with a large number of bacterial species found to have hydrophobic properties.[27] Unfortunately, many of the vital medical devices frequently used are made of materials that are hydrophobic, such as endotracheal tubes, catheters, and PICC lines making them more susceptible to biofilm formation.

1.4 Current Preventative Strategies

Aside from antibiotics, other measures are implemented to prevent and treat device-related infection in a clinical environment. Around 1999, there were more than 27 million surgical procedures performed each year in the US, all involving contact between the sterile patient's tissues and medical equipment.[28] Today, due to the increase in medical and technological advances, that number is closer to 50 million surgical procedures annually.[29] The first line of defense for infection prevention during these procedures is through sterilization of materials. Sterilization can be achieved by steam techniques, ethylene oxide gas, and radiation. These methods are highly successful at completely eliminating pathogens, but sterilized materials can quickly become vulnerable to contamination once removed from the sterile field. The ability to use sterilization techniques is also limited by the type of material. Some materials cannot withstand the high temperatures and pressures during the process. Even for materials that can withstand sterilization methods, when used in long-term situations contamination is inevitable.

With these limitations in mind, researchers have aimed to develop materials that can resist infection even after implantation. For example, urinary catheters are highly prone to biofilm build-up if used for extended durations. In fact, virtually all patients with an indwelling urinary catheter for more than 28 days developed an infection.[30] These biofilms and encrustations may then lead to device blockage and failure. With nearly 560,000 catheter-associated urinary tract infections reported annually, a new type of catheter was proposed that is coated with a silver hydrogel layer.[31] This technology was also translated to other indwelling medical devices, such as endotracheal tubes and central venous catheters.[32] Silver was chosen due to its innate antimicrobial properties and minimal bacteria resistance.[33] Silver's antimicrobial activity is multifaceted and attacks bacteria differently than standard antibiotics. In nanoparticle form, silver can disrupt bacteria cell wall function, penetrate the membrane, and generate reactive oxygen species (**Figure 1.2**).[34] This is also true for various other transition metal ions, such as zinc and copper.[35] Unfortunately, various clinical and laboratory-related studies have identified little to no difference between silver coated materials and controls.[36-38] Silver also causes increased platelet activation when exposed to blood, leading to an increased chanced of thrombus formation, even under the systemic effects of heparin.[39] The use of silver raises concerns over cytotoxicity effects and environmental implications.

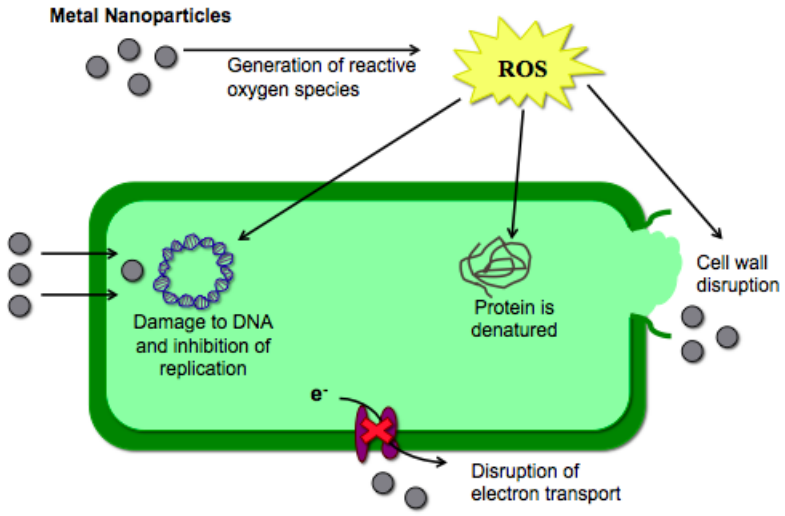

Figure 1.2. Various methods of metal ion antimicrobial action with bacteria cells. Most activity occurs through the generation of reactive oxygen species that can disrupt cell structures and function. Metal ions can also cross the cell membrane and directly damage cellular components.

Another area of study for preventing bacteria contamination and infection is through modification of indwelling medical device materials. A material's propensity to be bound by microbial organism is determined by its chemical composition, the site of implantation, surface characteristics, and mechanical interactions with host tissues.[21] Current strategies for resisting bacterial adhesion includes the selection of hydrophilic surfaces. Hydrophilic materials have the ability to form hydrogen bonds with water and allow for the formation of a hydration layer.[40] The layer acts as a physical barrier, passively protecting the material from planktonic bacteria adhesion, but plays no role in bacterial killing. Additional passive surfaces for reducing adhesion include cationic and zwitterionic charged coatings.[41] Drug-eluting materials are a more direct approach to preventing device-related infection. In particular, polymer systems that actively release antibiotics have been developed using vancomycin, gentamycin, amoxicillin, and

cephalothin.[42] By incorporating these antimicrobials directly within the material, high dosages of the drugs can be used to control infection in the area of the device. However, this strategy is limited by the capacity of the polymeric material and which pathogens a single antibiotic can target, as well as the potential to enable pathogenic resistance.

1.5 Background on Nitric Oxide

In an effort to address the need for new antimicrobial agents, researchers have turned to nitric oxide (NO), the endothelium-derived relaxation factor identified by Furchgott, Ignarro, and Murad in 1987.[16,43] This gaseous free radical molecule has been identified as a potent antimicrobial agent, mediator of smooth muscle relaxation and platelet inhibitor. In mammalian cells, NO is produced from the conversion of L-arginine to L-citrulline enzymatically by nitric oxide synthase (NOS) in the presence of molecular oxygen. NO can be generated by three different isoforms of NOS differentiated by their utilization of calcium. Endothelial NOS (eNOS) and neuronal NOS (nNOS) are calcium dependent and generate low, continuous levels of NO release, while inducible NOS (iNOS) is calcium independent and generates high levels of NO when needed.[44] Each isoform may be found in various areas of the body, with all three having regulatory roles in the cardiovascular system.[45]

NO's antimicrobial action functions by direct and indirect processes. Both pathways entail nitrosative and oxidative action. Directly, the small and virtually uncharged NO molecule can diffuse across membranes with relative ease. Once inside the bacteria cell NO can form reactive oxygen species intermediates *in situ* or directly target DNA and microbial proteins. In an indirect manner NO reacts with superoxide to produce a potent oxidizer intermediate, peroxynitrite ($OONO^-$). As with NO,

peroxynitrite can cross the bacterial membrane and target cellular components leading to enzyme inhibition, lipid peroxidation and protein nitrosation.[46,47] Peroxynitrite may also be formed through the reaction of additional NO analogs such as nitrous acid (HNO_2) with hydrogen peroxide (H_2O_2) or when nitroxyl (NO^-) reacts with oxygen.[48] Due to its broad spectrum of antimicrobial actions, NO has a reduced probability of microbial resistance. Typical antimicrobial molecules are not effective against biofilm bacteria due to the protective extracellular matrix that surrounds them. NO has been proven to be effective against biofilm bacteria in addition to planktonic bacteria, demonstrating the ability to disperse pre-existing *P. aeruginosa* and *E. coli* biofilms, putting the bacteria in a planktonic state and making them vulnerable to traditional antibiotic methods.[49,50]

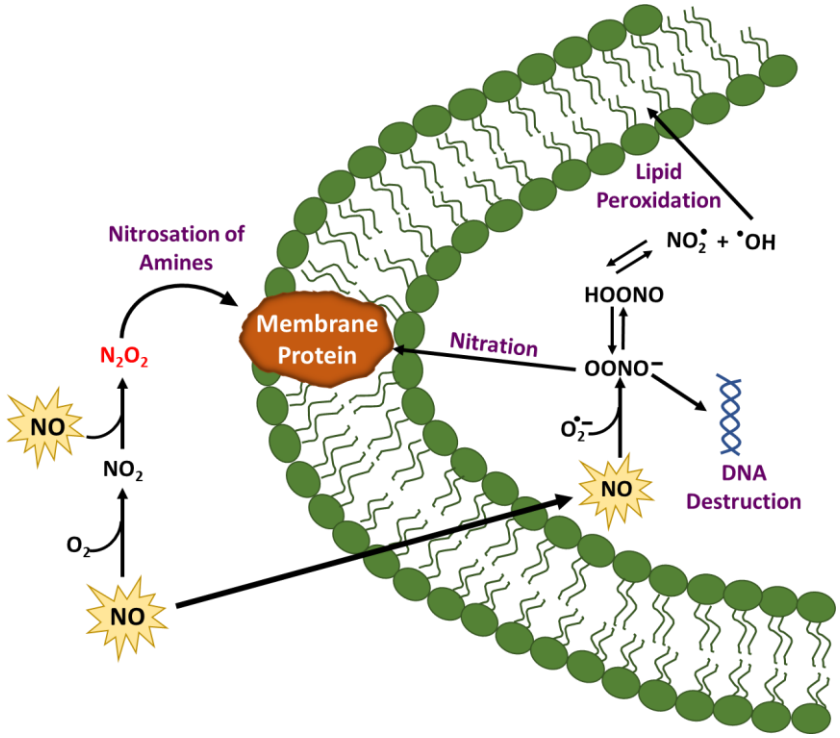

Figure 1.3. NO can indirectly and directly target bacterial cells. Directly, NO can cross the membrane and react with superoxide to produce peroxynitrite. Peroxynitrite can react with tyrosine on membrane proteins, as well as produce oxidizing agents.

Due to NO's enticing antimicrobial traits, NO donors have been developed to store, transport, and delivery NO to mimic the body's natural host defenses. The usage of NO in the form of a singularly gaseous molecule presents challenges with a short half-life *in vivo*, which led to the development of donor molecules. Some major classes of NO donors of particular focus are *S*-nitrosothiols, diazeniumdiolates, organic nitrates/nitrites, and metal-NO complexes. While these are the major donors researched for biomaterials, it is important to note that many compounds with nitrogen-oxygen bonds are capable of decomposing and generating reactive nitrogen species. Most donors release their NO payload as they decompose in the presence of light, moisture, and heat.[51] Some donors are pH dependent or require the addition of a catalyst.

Organic nitrates and nitrites have long been used in the cardiovascular field as therapeutic agents in the treatment of vascular and heart diseases, but are often limited by their short half-life and drug tolerance.[52] To overcome these limitations additional NO donors were sought leading to the emergence of the widely studied class of diazeniumdiolates (NONOates). The unique structure of NONOates allows for the molecule to covalently attach two moles of NO, however the instability of the molecule results in rapid release of its NO payload when placed in physiological pH and temperature, presenting challenges for long-term medical applications. A more recent class of NO donors with exciting potential are naturally occurring and synthetic *S*-nitrosothiols (RSNOs). When exposed to thermal conditions, a metal ion catalyst, or moisture, RSNOs can relinquish their NO group in the forms of $NO^{\bullet}$, NO^{-}, and NO^{+} through a heterolytic or homolytic cleavage.[44,53] One example of an endogenous RSNO is *S*-nitrosoglutathione (GSNO). GSNO is a stable NO carrier with important roles in NO

signaling pathways. A synthetic RSNO used extensively in preclinical studies and the focus of this thesis is *S*-nitroso-*N*-acetylpenicillamine, referred to as SNAP. SNAP has shown significant antimicrobial activity in both *in vitro* and *in vivo* studies.[20,54] A study of the shelf-life of a SNAP-doped material resulted in 87% retention of the initial SNAP content after 6 months at room temperature conditions, demonstrating its stability and potential for commercial use.[55] Compared to GSNO, the chemical nature of SNAP and its ability to be dissolved in a variety of organic solvents make it a more appealing molecule to use in many medical grade polymers.

Effective delivery of exogenous NO for therapeutic purposes is an important topic in the biomaterial field. Generally, researchers aim to design materials that are NO-releasing or materials that can generate NO from endogenous sources. When designing NO-releasing materials, the desired levels of NO surface flux rate are intended to match the physiologically levels of 0.5 – 4 x 10^{-10} mol min^{-1} cm^{-2} produced by the endothelium.[56] Recent work has shown that surfaces with a NO flux as low was 0.3 x 10^{-10} mol min^{-1} cm^{-2} were still effective at reducing viable bacteria attachment.[57] Release of NO is often controlled by the polymeric matrix chosen. A more hydrophilic polymer will lead to a more rapid release of NO by hydrolysis, where as a more hydrophobic polymer may release its NO content more consistently at lower levels. The release profile of NO is also determined by the donor chosen. For example, with SNAP-doped materials the release of NO is impacted by the crystallization of the SNAP molecule within the polymer matrix during material fabrication.[58] Crystallization tends to occur when the concentration of SNAP meets or exceeds 10 wt% of the polymer it is incorporated within.[55]

The fabrication of NO-releasing materials is accomplished through either physical blending or chemical attachment of the NO donor to the polymer. Selection of polymer is important for solvents that are also compatible with the NO donor. In cases of direct attachment, it is pertinent to maintain the integrity of the starting polymer. This can be determined through mechanical testing and property characterizations before and after attachment. Some examples of polymers used for direct attachment include polyvinyl chloride (PVC) and poly(dimethylsiloxane) (PDMS).[57,59] In cases of physical blending, retention of the NO donor is of concern and should be monitored through leaching studies. An additional approach to physical blending consists of solvent-swelling.[60] This approach is utilized in cases that require a polymer substrate to be heated for crosslinking, such as the case of catheters made using extrusion polymerization methods. The use of high heat can cause the NO donors to release their NO content and should be avoided. To circumvent this issue, placing the cured polymer in a solution of solvent/NO donor allows for the donor to infiltrate the swelled polymer matrix. The appropriate fabrication method and polymer should be selected based on the material application.

Materials that generate NO from endogenous sources are still in the early developmental phase but show great promise for maintaining an unending supply of NO. NO is generated *in vivo* through catalyzation of RSNOs, electrochemical reduction of nitrite, or reduction of sodium nitroprusside.[60] One research group has immobilized L-cysteine to a polyethylene terephthalate (PEG) polymer backbone in order to supply a free thiol to undergo a reaction with circulating nitrosothiols.[61] Others have used the catalytic approach by incorporating a lipophilic copper (II) complex to generate NO from

endogenous sources.[62] Both studies show promising outlooks, but there are still challenges in measuring NO generation *in vivo*.

While NO work shows promising results, the current fabrication methods have some drawbacks. These drawbacks include high cost of production, storage stability, and lifetime of NO release. Many methods fail to establish a controllable or sustained release rate and often exhaust their NO reservoir within the first 24 h when exposed to physiological conditions. Controlling NO levels is crucial for various biological functions and applications, which is why the versatility of using RNSO based donors like SNAP is necessary to improve the overall biocompatibility of medical devices. This thesis aims to address the current drawbacks of NO-releasing platforms and improve antimicrobial activity of these systems. Diverse novel methods are demonstrated that improve two types NO donor scaffolds, electrospun polyacrylonitrile (PAN) and polyurethane-silicone copolymer.

Chapter 2 of this thesis presents a method for enhancing NO release over an extended period of time. This is accomplished by the addition of a metal ion catalyst, in the form of zinc oxide nanoparticles, top-coated on a SNAP-impregnated polymer. Traditionally, polymers embedded with RSNOs do not release a high enough flux for a prolonged duration to be an effective antimicrobial surface. The incorporation of a zinc catalyst was able to enhance the NO release significantly. In addition to the improvement of NO release kinetics, the zinc ion adds an additional antimicrobial agent that allows for further broad-spectrum activity. The synergy between zinc and NO helped to significantly reduce the amount of viable bacteria adherence on the material surface, compared to either agent alone. Several additional studies were conducted to characterize

the multifaceted material, indicating a uniform zinc coating, low cytotoxicity to fibroblast, and minimal NO donor leaching.

A novel approach to fabricating NO-releasing nanofibers is discussed in Chapter 3. Directly blending polymeric fibers with an antimicrobial agent can result in rapid leaching of the agent and are not suitable for long-term applications. In cases of fibrous wound dressings, release rate of the antimicrobial agent is crucial in the reduction of the growth rate of bacteria within a wound.[63] To provide a more stable and longer-term release of NO in wound healing applications, we present a chemical method for the irreversible attachment of an RNSO donor directly to PAN nanofibers. Antimicrobial capabilities and wound healing resolution are both important parameters to consider when designing a wound healing scaffold, and the incorporation of NO release enhances both of these properties. By covalently attaching the donor to the polymer, the concern of leaching was eliminated, which in turn prolonged the NO release from the nanofibers. The newly fabricated SNAP-PAN fibers were evaluated for fibroblast attachment and proliferation, proving beneficial in the support of the wound healing process. Overall, this work demonstrates the improvement of NO-releasing nanofiber platforms for wound healing and infection prevention applications.

1.6 REFERENCES

1. Klevens RM, Edwards JR, Richards Jr CL, et al. Estimating health care-associated infections and deaths in US hospitals, 2002. *Public health reports.* 2007;122(2):160-166.

2. Magill SS, Edwards JR, Bamberg W, et al. Multistate point-prevalence survey of health care–associated infections. *New England Journal of Medicine.* 2014;370(13):1198-1208.

3. CDC. Preventing Healthcare-Associated Infections. *Centers for Disease Control and Prevention.*

4. Furno F, Morley KS, Wong B, et al. Silver nanoparticles and polymeric medical devices: a new approach to prevention of infection? *Journal of Antimicrobial Chemotherapy.* 2004;54(6):1019-1024.

5. Chastre J, Fagon J-Y. Ventilator-associated pneumonia. *American journal of respiratory and critical care medicine.* 2002;165(7):867-903.

6. Fair RJ, Tor Y. Antibiotics and bacterial resistance in the 21st century. *Perspectives in medicinal chemistry.* 2014;6:PMC. S14459.

7. Vertes A, Hitchins V, Phillips KS. Analytical challenges of microbial biofilms on medical devices: ACS Publications; 2012.

8. Miller MB, Bassler BL. Quorum sensing in bacteria. *Annual Reviews in Microbiology.* 2001;55(1):165-199.

9. Percival SL, Suleman L, Vuotto C, Donelli G. Healthcare-associated infections, medical devices and biofilms: risk, tolerance and control. *Journal of medical microbiology.* 2015;64(4):323-334.

10. Kourkouta L, Tsaloglidou A, Koukourikos K, Iliadis C, Plati P, Dimitriadou A. History of Antibiotics.

11. Levy SB, Marshall B. Antibacterial resistance worldwide: causes, challenges and responses. *Nature medicine.* 2004;10(12s):S122.

12. Ventola CL. The antibiotic resistance crisis: part 1: causes and threats. *Pharmacy and Therapeutics.* 2015;40(4):277.

13. Gosbell IB. Methicillin-resistant Staphylococcus aureus. *American journal of clinical dermatology.* 2004;5(4):239-259.

14. Tenover FC, Pearson ML. Methicillin-resistant Staphylococcus aureus.(1). *Emerging infectious diseases.* 2004;10(11):2052-2054.

15. Naik K, Srivastava P, Deshmukh K, Monsoor S, Kowshik M. Nanomaterial-based approaches for prevention of biofilm-associated infections on medical devices and implants. *Journal of nanoscience and nanotechnology.* 2015;15(12):10108-10119.

16. Carpenter AW, Schoenfisch MH. Nitric oxide release: Part II. Therapeutic applications. *Chemical Society Reviews.* 2012;41(10):3742-3752.

17. Williams DF. On the mechanisms of biocompatibility. *Biomaterials.* 2008;29(20):2941-2953.

18. Morais JM, Papadimitrakopoulos F, Burgess DJ. Biomaterials/tissue interactions: possible solutions to overcome foreign body response. *The AAPS journal.* 2010;12(2):188-196.

19. Anderson JM, Rodriguez A, Chang DT. FOREIGN BODY REACTION TO BIOMATERIALS. *Seminars in immunology.* 12/26 2008;20(2):86-100.

20. Pant J, Goudie MJ, Chaji SM, Johnson BW, Handa H. Nitric oxide releasing vascular catheters for eradicating bacterial infection. *Journal of Biomedical Materials Research Part B: Applied Biomaterials.* 2017.

21. An YH, Friedman RJ. *Handbook of bacterial adhesion: principles, methods, and applications.* Vol 204: Springer Science & Business Media; 2000.

22. Merritt K, Chang C. Factors influencing bacterial adherence to biomaterials. *Journal of biomaterials applications.* 1991;5(3):185-203.

23. Duddridge JE, Kent C, Laws J. Effect of surface shear stress on the attachment of Pseudomonas fluorescens to stainless steel under defined flow conditions. *Biotechnology and bioengineering.* 1982;24(1):153-164.

24. Absolom DR, Lamberti FV, Policova Z, Zingg W, van Oss CJ, Neumann AW. Surface thermodynamics of bacterial adhesion. *Applied and environmental microbiology.* 1983;46(1):90-97.

25. An YH, Friedman RJ. Concise review of mechanisms of bacterial adhesion to biomaterial surfaces. *Journal of biomedical materials research.* 1998;43(3):338-348.

26. Vacheethasanee K, Temenoff JS, Higashi JM, et al. Bacterial surface properties of clinically isolated Staphylococcus epidermidis strains determine adhesion on polyethylene. *Journal of Biomedical Materials Research: An Official Journal of The Society for Biomaterials, The Japanese Society for Biomaterials, and the Australian Society for Biomaterials.* 1998;42(3):425-432.

27. Doyle RJ. Contribution of the hydrophobic effect to microbial infection. *Microbes and infection.* 2000;2(4):391-400.

28. Rutala WA, Weber DJ. Draft guideline for disinfection and sterilization in healthcare facilities. *Centers for Disease Control and Prevention, Atlanta, GA.* 2002.

29. Hall MJ, Schwartzman A, Zhang J, Liu X. Ambulatory surgery data from hospitals and ambulatory surgery centers: United States, 2010. *National health statistics reports.* 2017(102):1-15.

30. Donlan RM. Biofilms and device-associated infections. *Emerging infectious diseases.* 2001;7(2):277.

31. Medicare Cf, Services M. CMS proposes additions to list of hospital-acquired conditions for fiscal year 2009. *Available at:)(Accessed July 15, 2008) View in Article| Google Scholar.* 2012.

32. Politano AD, Campbell KT, Rosenberger LH, Sawyer RG. Use of silver in the prevention and treatment of infections: silver review. *Surgical infections.* 2013;14(1):8-20.

33. Rai M, Yadav A, Gade A. Silver nanoparticles as a new generation of antimicrobials. *Biotechnology advances.* 2009;27(1):76-83.

34. Marambio-Jones C, Hoek EM. A review of the antibacterial effects of silver nanomaterials and potential implications for human health and the environment. *Journal of Nanoparticle Research.* 2010;12(5):1531-1551.

35. Turner RJ. Metal-based antimicrobial strategies. *Microbial biotechnology.* 2017;10(5):1062-1065.

36. Björling G, Johansson D, Bergström L, et al. Tolerability and performance of BIP endotracheal tubes with noble metal alloy coating–a randomized clinical evaluation study. *BMC anesthesiology.* 2015;15(1):174.

37. Bonfill X, Rigau D, Esteban-Fuertes M, et al. Efficacy and safety of urinary catheters with silver alloy coating in patients with spinal cord injury: a multicentric pragmatic randomized controlled trial. The ESCALE trial. *The Spine Journal.* 2017;17(11):1650-1657.

38. Desai DG, Liao KS, Cevallos ME, Trautner BW. Silver or nitrofurazone impregnation of urinary catheters has a minimal effect on uropathogen adherence. *The Journal of urology.* 2010;184(6):2565-2571.

39. Stevens KN, Crespo-Biel O, van den Bosch EE, et al. The relationship between the antimicrobial effect of catheter coatings containing silver nanoparticles and the coagulation of contacting blood. *Biomaterials.* 2009;30(22):3682-3690.

40. Chen S, Li L, Zhao C, Zheng J. Surface hydration: principles and applications toward low-fouling/nonfouling biomaterials. *Polymer.* 2010;51(23):5283-5293.

41. Harding JL, Reynolds MM. Combating medical device fouling. *Trends in biotechnology.* 2014;32(3):140-146.

42. Hetrick EM, Schoenfisch MH. Reducing implant-related infections: active release strategies. *Chemical Society Reviews.* 2006;35(9):780-789.

43. Ignarro LJ, Buga GM, Wood KS, Byrns RE, Chaudhuri G. Endothelium-derived relaxing factor produced and released from artery and vein is nitric oxide. *Proceedings of the National Academy of Sciences.* 1987;84(24):9265-9269.

44. Pant J, Goudie M, Brisbois E, Handa H. Nitric oxide-releasing polyurethanes. *Advances in Polyurethane Biomaterials*: Elsevier; 2016:417-449.

45. Förstermann U, Sessa WC. Nitric oxide synthases: regulation and function. *European heart journal.* 2011;33(7):829-837.

46. De Groote MA, Fang FC. NO inhibitions: antimicrobial properties of nitric oxide. *Clinical Infectious Diseases.* 1995;21(Supplement_2):S162-S165.

47. Schairer DO, Chouake JS, Nosanchuk JD, Friedman AJ. The potential of nitric oxide releasing therapies as antimicrobial agents. *Virulence.* 2012;3(3):271-279.

48. Fang FC. Perspectives series: host/pathogen interactions. Mechanisms of nitric oxide-related antimicrobial activity. *The Journal of clinical investigation.* 1997;99(12):2818-2825.

49. Barraud N, Hassett DJ, Hwang S-H, Rice SA, Kjelleberg S, Webb JS. Involvement of nitric oxide in biofilm dispersal of Pseudomonas aeruginosa. *Journal of bacteriology.* 2006;188(21):7344-7353.

50. Barraud N, J Kelso M, A Rice S, Kjelleberg S. Nitric oxide: a key mediator of biofilm dispersal with applications in infectious diseases. *Current pharmaceutical design.* 2015;21(1):31-42.

51. Wang PG, Xian M, Tang X, et al. Nitric oxide donors: chemical activities and biological applications. *Chemical reviews.* 2002;102(4):1091-1134.

52. Ignarro LJ, Napoli C, Loscalzo J. Nitric oxide donors and cardiovascular agents modulating the bioactivity of nitric oxide: an overview. *Circulation research.* 2002;90(1):21-28.

53. Maron BA, Tang S-S, Loscalzo J. S-nitrosothiols and the S-nitrosoproteome of the cardiovascular system. *Antioxidants & redox signaling.* 2013;18(3):270-287.

54. Wo Y, Brisbois EJ, Wu J, et al. Reduction of Thrombosis and Bacterial Infection via Controlled Nitric Oxide (NO) Release from S-Nitroso-N-acetylpenicillamine (SNAP) Impregnated CarboSil Intravascular Catheters. *ACS biomaterials science & engineering.* 2017;3(3):349-359.

55. Goudie MJ, Brisbois EJ, Pant J, Thompson A, Potkay JA, Handa H. Characterization of an S-nitroso-N-acetylpenicillamine–based nitric oxide releasing polymer from a translational perspective. *International Journal of Polymeric Materials and Polymeric Biomaterials.* 2016;65(15):769-778.

56. Vaughn MW, Kuo L, Liao JC. Estimation of nitric oxide production and reactionrates in tissue by use of a mathematical model. *American Journal of Physiology-Heart and Circulatory Physiology.* 1998;274(6):H2163-H2176.

57. Hopkins SP, Pant J, Goudie MJ, Schmiedt C, Handa H. Achieving long-term biocompatible silicone via covalently immobilized S-nitroso-N-acetylpenicillamine (SNAP) that exhibits 4 months of sustained nitric oxide release. *ACS applied materials & interfaces.* 2018.

58. Wo Y, Li Z, Colletta A, et al. Study of crystal formation and nitric oxide (NO) release mechanism from S-nitroso-N-acetylpenicillamine (SNAP)-doped CarboSil polymer composites for potential antimicrobial applications. *Composites Part B: Engineering.* 2017;121:23-33.

59. Hopkins S, Frost M. Synthesis and Characterization of Controlled Nitric Oxide Release from S-Nitroso-N-Acetyl-d-Penicillamine Covalently Linked to Polyvinyl Chloride (SNAP-PVC). *Bioengineering.* 2018;5(3):72.

60. Colletta A, Wu J, Wo Y, et al. S-Nitroso-N-acetylpenicillamine (SNAP) impregnated silicone foley catheters: a potential biomaterial/device to prevent catheter-associated urinary tract infections. *ACS biomaterials science & engineering.* 2015;1(6):416-424.

61. Frost MC, Reynolds MM, Meyerhoff ME. Polymers incorporating nitric oxide releasing/generating substances for improved biocompatibility of blood-contacting medical devices. *Biomaterials.* 2005;26(14):1685-1693.

62. Oh BK, Meyerhoff ME. Spontaneous Catalytic Generation of Nitric Oxide from S-Nitrosothiols at the Surface of Polymer Films Doped with Lipophilic Copper(II) Complex. *Journal of the American Chemical Society.* 2003/08/01 2003;125(32):9552-9553.

63. Zahedi P, Rezaeian I, Ranaei-Siadat SO, Jafari SH, Supaphol P. A review on wound dressings with an emphasis on electrospun nanofibrous polymeric bandages. *Polymers for Advanced Technologies.* 2010;21(2):77-95.

CHAPTER 2

ENHANCED ANTIMICROBIAL AND CATALYTIC EFFECT OF ZINC OXIDE NANOPARTICLES TOPCOATED ON A NITRIC OXIDE RELEASING POLYMER[1]

[1] Priyadarshini Singha, Christina D. Workman, Jitendra Pant, Sean Hopkins, Hitesh Handa. Submitted to *SFB's Journal of Biomedical Materials Research Part A.* October 2018.

ABSTRACT

The development of infection resistant materials is of foremost importance as seen with an increase in antibiotic resistance. In this project, the NO-releasing polymer has an added topcoat of zinc oxide nanoparticle (ZnO-NP) to improve NO release and match the endogenous NO flux ($0.5 – 4 \times 10^{-10}$ mol cm^{-2} min^{-1}). The ZnO-NP is incorporated to act as a catalyst and provide the additional benefit of acting synergistically with NO as an antimicrobial agent. The ZnO-NP topcoat is applied on a polycarbonate-based polyurethane (CarboSil) that contains blended NO donor, *S*-nitroso-*N*-acetylpenicillamine (SNAP). This sample, SNAP-ZnO, continuously had NO release above 0.5×10^{-10} mol cm^{-2} min^{-1} for 14 days while samples containing only SNAP dropped below physiological levels within 24 hours. The ZnO-NP topcoat improved NO release and reduced the amount of SNAP leached by 55% over a 7-day period. ICP-MS data observed negligible Zn ion release into the environment, suggesting longevity of the catalyst within the material. Compared to CarboSil films, the SNAP-ZnO films had a 99.03% killing efficacy against *S. aureus* and 87.62% killing efficacy against *P. aeruginosa*. A cell cytotoxicity study using mouse fibroblast 3T3 cells also noted no significant difference in viability between the controls and the SNAP-ZnO material, indicating no toxicity towards mammalian cells. The studies indicate that the synergy of combining a metal ion catalyst with a NO-releasing polymer significantly improved NO release kinetics and antimicrobial activity for device coating applications.

2.1 INTRODUCTION

One of the most common problems with implanted medical devices is the increased susceptibility of the patients to infections.[1] Infections attributed to medical devices, otherwise known as healthcare associated infections (HAIs), have led to various complications like increased healthcare costs, medical device failure, and unnecessary deterioration in a patient's health.[2] While the Center for Disease Control and Prevention estimates that 1 out of every 25 hospitalized patients is affected, HAIs are increasingly linked to mortality and morbidity.[3] Some of the most common types of HAIs include catheter associated urinary tract infections, surgical site infections, and bloodstream infections. The need to prevent and control HAIs is evident; such infections can be transmitted between different healthcare facilities and their prevention can result up to $31.5 billion in medical cost savings.[3]

While infection can be managed using several strategies, prevention of infection by anti-fouling and antimicrobial materials for medical devices has been studied extensively.[4] Although some of the most successful strategies include both active and passive agents, active agents are most widely studied due to their higher rate of success in preventing infections in the long term, whereas passive surfaces can be fail over time. Passive materials such as polyethyl glycol, zwitterionic polymers and other hydrophilic polymers are unable to kill the pathogens themselves and can also be fouled over time through settling of other biomacromolecules, which in turn can attract microbes. Therefore, agents such as silver nanoparticles (Ag-NPs), antibiotics, chlorhexidine, triclosan, quaternary ammonium ions, antimicrobial peptides, and nitric oxide (NO) have been studied widely.[5]

The often miraculous and controversial roles of nitric oxide (NO) in several biological applications from nerve signals to gut functions have been studied aggressively since 1992 when it was awarded the "Molecule of the Year" by The American Association for the Advancement of Science. Since NO's half-life is very short in physiological conditions, NO is transported in the form of endogenous S-nitrosothiols (RSNOs, e.g. S-nitrosoglutathione (GSNO), S-nitrosoalbumin, S-nitrosocysteine).[6] S-nitrosothiols degrade to release NO and result in disulfide formation.[7] However, over the last two decades, NO release from both endogenous and synthetic donors has been studied for the purpose of antimicrobial medical device coatings and wound healing applications.[5,8-14] While a couple of NO donors like N-diazeniumdiolates,[15-17] and S-nitrosothiols [18,19] have been researched extensively, their disadvantages include low NO release, cytotoxicity towards mammalian cells, and by-products that are not approved by the FDA. Similar to GSNO, SNAP is another RSNO, but is synthetic and has a longer shelf-life with increased NO donor capacity in polymers.[20] SNAP has been studied extensively in different polymers and thus is a well-characterized NO donor with the least cytotoxicity towards mammalian cells since the release of NO leads to FDA approved by-products.[21]

Zinc oxide is another antimicrobial but it is already commercially used and is known to have less cytotoxicity towards mammalian cells while having similar antibacterial effects at the same concentration when compared to other commonly used antimicrobial metal ions such as copper and silver.[22] It has been shown to inhibit the growth of dental caries-related bacteria, *Streptococcus mutans*, *Actinomyces viscosus*, *Lactobacillus casei*, *Staphylococcus aureus (S. aureus)*, and *Candida albicans.*[23] Zinc

oxide nanoparticles (ZnO-NPs) have been found to inhibit growth and cause loss of cell viability in *Escherichia coli (E. coli)* and *S. aureus* at concentrations ranging from as low as 1 mM up to 3.4 mM. The same concentrations also had minimal effects on primary human T cell viability.[24] Metal ions with high affinity for sulfur like Zn ions tend to inhibit glycolysis within microorganisms by oxidizing thiols groups in essential glycolytic enzymes. Coupled with low toxicity towards mammalian cells, ZnO-NPs are a good example of metal ion nanoparticles that are required in low concentrations for increased antimicrobial effects.[25]

As of yet, no studies have been conducted to demonstrate the improvement of antimicrobial activity of biomaterials that contain *both* NO releasing properties and ZnO-NP coated surfaces. The hybrid material fabricated in this study containing both ZnO-NP and NO donor capacity will serve two purposes: 1) provide a synergistic effect of antimicrobial properties by combining different mechanisms of bactericidal properties exhibited by NO and ZnO -NPs, and 2) ZnO-NPs would provide a catalytic platform for NO release.

While the enhanced biological effects of nitric oxide releasing materials have been studied with metal ions like iron and copper,[26-28] and polyurethane/metal organic framework composite materials,[29] the catalytic effects of a much more mammalian cell friendly metal ion, ZnO-NPs, has not been studied *until now*. In the past, the effect of Zn^{2+} on its ability to generate NO from SNAP has been studied using a Zn wire and a solution for *in vivo* biodegradable bare stent and has been found to elevate NO release.[30]

However, the enhanced biological effects, like increased antimicrobial activity and lower cytotoxic effects of ZnO-NPs on NO releasing polymers have not been studied.

As discussed herein, we have attempted to fabricate, study, and demonstrate the catalytic and antimicrobial properties of a hybrid material **SNAP-ZnO** (**Figure 2.1**). ZnO-NPs were topcoated on a NO-releasing polymer to enhance infection resistant properties of potential medical coatings. Different concentrations of ZnO-NPs were dispersed in previously established concentrations of NO-releasing polymer topcoats and studied for leaching properties of SNAP. Once the least leaching (highest SNAP storage) combination is determined, the hybrid sample is then used to investigate synergistic properties of NO and ZnO-NP in antimicrobial and cytotoxicity studies. Studies for up to 14 days of elevated NO release and 24-hour antimicrobial effects have been presented. Along with proving the antimicrobial efficacy of the material, cytotoxic studies are performed to ensure mammalian cell friendly nature of the final product.

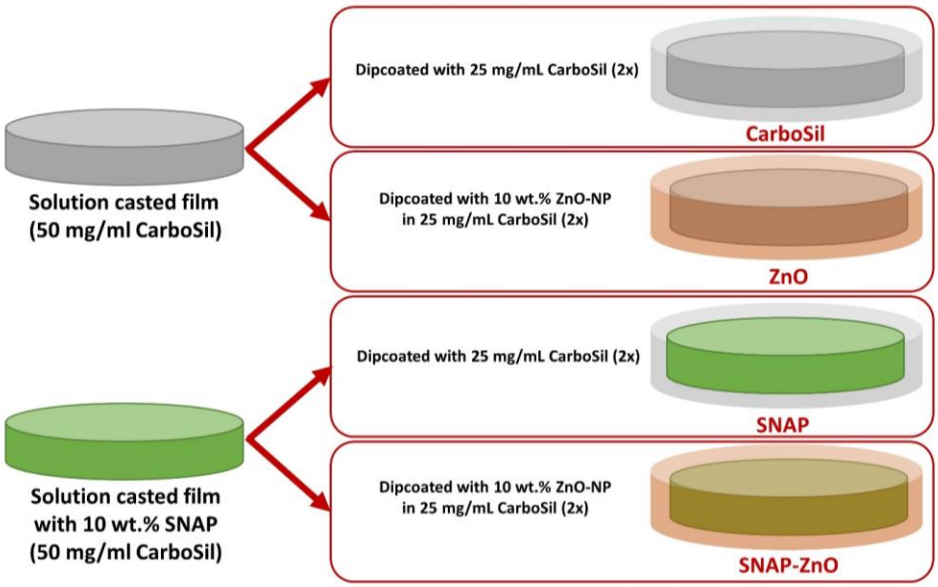

Figure 2.1. Fabrication process of four main tested samples in antimicrobial and cytotoxicity tests. CarboSil, ZnO, SNAP, SNAP-ZnO**.**

2.2 MATERIALS AND METHODS

Materials

CarboSil® 2080A UR STPU (referred to as CarboSil hereon) was acquired from DSM Biomedical Inc. (Berkeley, CA). Anhydrous tetrahydrofuran (THF), *N*-acetyl-*D*-penicillamine (NAP), sodium nitrite ($NaNO_2$), concentrated sulfuric acid (H_2SO_4), phosphate buffered saline (PBS), ZnO-NPs, cell counting kit-8 and ethylenediamine tetraacetic acid (EDTA) were obtained from Sigma Aldrich (St. Louis, MO). Concentrated hydrochloric acid (conc. HCl), and methanol were bought from Fisher-Scientific (Hampton, NH). CarboSil™ 2080A (CarboSil) was obtained from DSM Biomedical Inc. (Berkeley, CA). Gram-positive *Staphylococcus aureus* (ATCC 6538) and Gram-negative *Pseudomonas aeruginosa* (ATCC 27853, *P. aeruginosa*) were originally obtained from American Type Culture Collection (Manassas, VA). Milli-Q filter was used to obtain deionized (DI) water for all the aqueous solution preparations. Nitrogen and oxygen gas cylinders were purchased from Airgas (Kennesaw, GA). LB Agar (LA), Miller and Luria broth (LB), Lennox were purchased from Fischer BioReagents (Fair Lawn, NJ).

Synthesis of S-nitroso-N-acetyl-penicillamine (SNAP)

The protocol for the synthesis of SNAP was followed from a previously reported method with slight modifications.[31] Briefly, 2M HCl and 2M H_2SO_4 were added to a beaker containing a 1:1 mixture by volume of methanol and water, followed by an equimolar ratio of NAP and $NaNO_2$. The solution was stirred for 30 minutes then moved to an ice bath to facilitate the precipitation of the SNAP crystals. After 6 hours, the crystals were collected via vacuum filtration and dried for 24 hours. The entire process

and crystals obtained were shielded from light throughout the entire duration of the experiment.

Fabrication of ZnO-NP loaded-NO Releasing Films

The bulk of the films were made using solvent casting method and top coats were added using dip coating (both techniques have been previously described and published).[31,32] Briefly, SNAP films were prepared by dissolving CarboSil in THF for a final concentration of 50 mg ml^{-1}. CarboSil is a polycarbonate-based polyurethane that contains a silicone segment and is marketed by DSM. It has been used previously by our and other groups and has been found to have good NO-releasing properties.[31-33] (Exact properties are not public knowledge but all details are available on the company's website.) When CarboSil was fully dissolved, 10 wt.% SNAP was added to the solution. The solution was then poured into a Teflon™ mold and left to dry in the dark, overnight. Dried films were cut into circular disks with diameters of 8 mm. Then, various solutions of 25 mg ml^{-1} of CarboSil were prepared separately (containing 0, 1, 5, and 10 wt.% ZnO-NP). The circular films were top coated twice with the prepared solution containing 0, 1,5 or 10 wt.% ZnO-NP by dipping the films in the solution and allowing 10 minutes of drying between coats. The ZnO-NP used was purchased from Sigma-Aldrich. The size of the ZnO-NP was specified as <50nm in size and >97% purity. All films were allowed 24 hours to fully dry before being used for experiments. Following is a table (**Table 2.1**) for all the compositions used along with the sample names.

Table 2.1. Composition for each sample.

Sample Fabrication		
SAMPLE NAME	**BASE FILM**	**TOPCOAT**
CarboSil	50 mg/ml CarboSil	2 dips of 25 mg/ml CarboSil solution
ZnO-1	50 mg/ml CarboSil	2 dips of 25 mg/ml CarboSil solution containing 1 wt.% ZnO-NP
ZnO-5	50 mg/ml CarboSil	2 dips of 25 mg/ml CarboSil solution containing 5 wt.% ZnO-NP
ZnO	50 mg/ml CarboSil	2 dips of 25 mg/ml CarboSil solution containing 10 wt.% ZnO-NP
SNAP	50 mg/ml CarboSil with 10 wt.% SNAP	2 dips of 25 mg/ml CarboSil solution
SNAP-ZnO-1	50 mg/ml CarboSil with 10 wt.% SNAP	2 dips of 25 mg/ml CarboSil solution containing 1 wt.% ZnO-NP
SNAP-ZnO-5	50 mg/ml CarboSil with 10 wt.% SNAP	2 dips of 25 mg/ml CarboSil solution containing 5 wt.% ZnO-NP
SNAP-ZnO	50 mg/ml CarboSil with 10 wt.% SNAP	2 dips of 25 mg/ml CarboSil® solution containing 10 wt% ZnO-NP

SNAP Leaching Analysis

Prepared circular films were tested for leaching of SNAP using UV-Vis spectrophotometry. The SNAP leached into the PBS used to soak the films was measured by detecting the absorbance at 340 nm wavelength (maximum absorbance for SNO bond in SNAP) at various time points over 7 days. Samples were weighed before applying the topcoats to determine the amount of SNAP initially present. After application of topcoats, films were soaked in PBS (with EDTA) at 37°C for the duration of the study. Measurements were compared to a calibration curve.

Energy-dispersive X-ray spectroscopy

Scanning electron microscopy (SEM, FEI Teneo, FEI Co.) fitted with a large detector Energy dispersive X-ray spectroscopy (EDS, Oxford Instruments) system was

employed at an accelerating voltage of 10.00 kV to examine the presence and elemental mapping of SNAP and ZnO-NP particles throughout the surfaces fabricated.

Nitric Oxide Release Measurements

Chemiluminescence of NO release from SNAP-ZnO films versus the SNAP films was measured using a Siever's Nitric Oxide Analyzer (NOA) (Boulder, CO). Films containing SNAP (both with and without ZnO coatings) were measured for their NO release. Each sample was placed in cell containing PBS buffer at 37°C. EDTA was added to this PBS buffer as a chelating agent and prevent any catalytic release of NO by free metal-ions in the solution. Nitrogen gas was bubbled through the solution to purge NO from the solution. Sweep gas carried the purged NO to the detection chamber, where it was measured in PPB. Samples were measured with NOA on day 0, 1, 3, 5, and 7. Between measurements samples were kept in PBS buffer in 37°C incubator.

Inductively Coupled Plasma – Mass Spectroscopy (ICP-MS)

To measure the amount of metal-ion nanoparticles (ZnO in this case) in the sample leachates for the duration of the study, an ICP-MS study was conducted using a VG ICP-MS Plasma Quad 3 instrument.[26] In this study, the samples containing ZnO topcoats were soaked in DMEM for 2 weeks and kept in 37°C. At the end of 2 weeks, the films were removed from the media and the media was analyzed for presence of ^{64}Zn and ^{66}Zn isotopes using a previously published method.[34]

Bacterial Adhesion Study

Bacterial adhesion study for the fabricated materials was carried out using a previously established ASTM E2180 protocol.[32] This protocol was performed with very

minor modifications. The samples used for the bacterial adhesion study were CarboSil, ZnO, SNAP and SNAP-ZnO. The bacteria used for antimicrobial efficacy analyses were *S. aureus* and *P. aeruginosa*. The bacteria were grown to a mid-log phase of ~10^6-10^8 CFU ml^{-1} in LB broth at 37°C. Following this, the bacteria were then resuspended in PBS to incubate the samples. 2 ml of bacterial solution was used for each sample and kept in a shaker incubator (37C, 200 rpm) for 24 h. After 24 h of incubation with the bacteria, samples were rinsed with DI water to remove any unattached bacteria. The samples were then homogenized for 1 min each to remove any adhered bacteria into buffer solutions. The buffer solutions, now containing bacteria from the materials, were serially diluted (up to 10^{-5}), plated on LB agar, and kept in the incubator (37°C). The colonies of bacteria were counted after 18 h of incubation and average number of CFUs were normalized for the surface area of each sample exposed to the bacteria.

Cytotoxicity Analysis

The cytotoxicity test was performed on mouse fibroblast cells (3T3) using a recommended and previously published cell cytotoxicity assay.[26] The mouse fibroblast cells were cultured from a cryopreserved vial Dulbecco's Modified Eagle's Media (DMEM) containing 5% glucose, 10% Fetal bovine serum and 1% antibiotics (Penn-Strep). The culture media was changed every second day until the cell confluency was 80-90%. After this step, 100 µl of 5000 cells/ml were seeded per well of a cell culture grade 96-well plate (n=5) and kept in a humidified incubator with 5% CO_2 maintained at 37°C.

In the meanwhile, leachates from the CarboSil films, SNAP-CarboSil, ZnO-CarboSil and ZnO-SNAP-CarboSil films were collected by adding 10 mg of each type of sample in 10 ml of DMEM media (n=5 for each sample type). The resulting mixture was covered in an amber vial in the incubator at 37°C for 24 hours to allow the films to leach in the DMEM medium.

After 24 hours, 10 µL of the leachates were added to each of the well-containing cells followed by incubation for 24 hours in the incubator. 10 µL of the WST-8 solution (CCK-8 kit, Sigma Aldrich) was added to the resulting mixture and incubated for 4 hours according to the manufacturer's recommendation. The NADH released by only viable fibroblast cells converted WST-8 to formazan, an orange color product that was quantified at 430 nm using a photo plate reader. The relative viability of the cells was measured with respect to CarboSil (cells exposed to CarboSil leachates) using the formula below.

$$\%\ \text{Cell Viability} = \frac{\text{Absorbance of the test samples}}{\text{Absorbance of the CarboSil samples}} \times 100$$

Statistical Analysis

All data are stated as mean ± standard deviation. The number of replicates for every experiment have been mentioned under methods used. Student's t-tests were performed with unequal variances and significance is reported as $p \leq 0.05$.

2.3 RESULTS AND DISCUSSION

Film Fabrication, Surface Characterization and NO Release Kinetics

Previous work has shown SNAP-blended polymers to release NO on the low end of the physiological range.[21] This is in part due to the need for hydrophobic polymers requiring a thin top coat as a support for SNAP to prevent rapid leaching of the molecule. The hydrophobicity of these polymers delays or prevents moisture from reaching the SNAP molecule to elicit NO release. We hypothesized that the addition of a metal ion, specifically Zn, would catalytically increase NO release from SNAP within the hydrophobic polymers without unnecessary SNAP leaching. For this study we used a biocompatible, medical grade thermoplastic urethane copolymer, CarboSil, as a support for SNAP.

Films of varying ZnO-NPs were made to test for SNAP leaching on consistent SNAP content films as mentioned on Table 1. This was done to establish the wt.% of ZnO-NP required for a longer NO-release with ideal SNAP storage. The amount of SNAP, 10 wt.%, required for sustained NO release has already been established in previously published results.[32] To determine if ZnO-NP topcoated films helped to retain SNAP within the film, a 7-day study on films stored in PBS (pH of 7.4, 37°C) was conducted. It is ideal to have high SNAP retention within the polymer in order to ensure prolonged NO release from the material, as well as avoid adverse cytotoxic effects, if any exist. After 7 days of soaking, all film types showed a high amount of SNAP retention (**Figure 2.2, Table 2.2**). Minimal leaching was demonstrated in the SNAP-ZnO films with only 7.75 ± 0.51 wt.% SNAP leached after 7 days, while films containing only

SNAP had the most SNAP leached (13.86 ± 3.62 wt.%). This higher retention of SNAP within SNAP-ZnO may be contributed to the ZnO-NP content in the topcoat as everything else is left consistent along the tested samples. The metal ion -blended topcoat may slow SNAP's ability to pass through the polymer layer. The catalytic effect of the ZnO-NP within the topcoat could also be facilitating a quicker degradation of the SNAP as it diffuses, resulting in the leaching of NAP instead which would be undetectable at the measured SNAP UV wavelength (340 nm). However, since NAP has been demonstrated in the past to be noncytotoxic and is even used in heavy metal chelation therapy, the possible leaching of this would not be problematic.[35] Due to these results all subsequent studies (NO Release measurement, EDS mapping, Antibacterial efficacy, Cytotoxicity) were performed with SNAP-ZnO as the proposed hybrid material demonstrated reduced loss of SNAP from the material despite having the exact same coatings as the other materials and differing only in the ZnO-NP content (10 wt.% compared to 1 and 5).

(Note: The loading efficiency of SNAP in all the films with SNAP is estimated to be ~100% since the SNAP crystals are allowed to dissolve and blend into the polymer/THF solution and casted into the molds.)

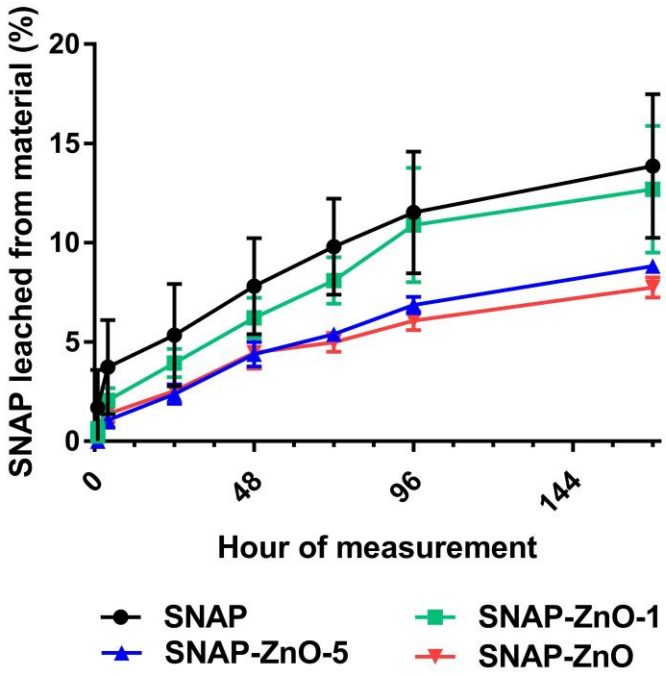

Figure 2.2. SNAP leaching profile for SNAP, SNAP-ZnO-1, SNAP-ZnO-5, and SNAP-ZnO-10 films. SNAP leaching was tested over 7 days/168 hours. (n=3)

Table 2.2. Complementary table for Figure 2: Weight percentage of SNAP leached.

	Wt. % of SNAP Leached						
	1 hour	**4 hours**	**24 hours**	**48 hours**	**72 hours**	**96 hours**	**168 hours**
SNAP	1.70 ±1.55	3.73 ±1.94	5.34 ±2.11	7.81 ±1.98	9.81 ±1.98	11.53±2.51	13.86 ±2.96
SNAP-ZnO-1	0.45 ±0.40	2.06 ±0.50	3.94 ±0.59	6.22 ±0.83	8.10 ±0.96	10.89 ±2.35	12.70 ±2.61
SNAP-ZnO-5	0.00 ±0.00	1.06 ±0.32	2.37 ±0.41	4.39 ±0.51	5.39 ±0.26	6.86 ±0.34	8.82 ±0.26
SNAP-ZnO	0.21 ±0.30	1.38 ±0.34	2.52 ±0.30	4.47 ±0.66	4.99 ±0.39	6.08 ±0.40	7.75 ±0.41

The low water uptake property of CarboSil allows for SNAP crystal formation within the polymer matrix. Exceeding the SNAP solubility threshold allows for crystallization of the molecule, thus stabilizing the NO donor to increase longevity of NO release.[36,37] To reach the optimum crystallization of SNAP without sacrificing mechanical properties of the polymer, 10 wt.% SNAP was used in all films, as

determined from previous work.[37] It was observed that the NO flux for the SNAP-ZnO films remained in the physiological range released from the endothelium of 0.5 to 4.0 ($x10^{-10}$ mol min^{-1} cm^{-2} for over 14 days (**Figure 2.3, Table 2.3**). While the SNAP samples had an initial burst (Day 0 not included in figure) in NO flux of 3.57 ± 0.814 ($x10^{-10}$ mol min^{-1} cm^{-2}), within 24 hours the flux was 0.24 ± 0.045 ($x10^{-10}$ mol min^{-1} cm^{-2}) and below 0.10 ($x10^{-10}$ mol min^{-1} cm^{-2}) by day 14. Although the average NO Flux for the SNAP-ZnO films on day 14 was 0.487 ± 0.075 ($x10^{-10}$ mol min^{-1} cm^{-2}), just below physiological levels, recent work has shown these levels still exhibit an antimicrobial effect.[38] The extended and improved NO release from SNAP-ZnO films shows a promising outlook for long-term indwelling medical device applications to reduce device-associated infections.

Table 2.3. Complementary table for Release of NO ($x10^{-10}$ mol cm^{-2} min^{-1}) from SNAP films vs. SNAP-ZnO films for 14 days.

	Day 1	Day 3	Day 5	Day 7	Day 11	Day 14
SNAP	0.241 ±0.045	0.222 ±0.023	0.235 ±0.084	0.203 ±0.048	0.123 ±0.061	0.079 ±0.043
SNAP-ZnO	2.766 ±0.427	1.752 ±0.145	1.253 ±0.129	0.851 ±0.019	0.649 ±0.026	0.487 ±0.075

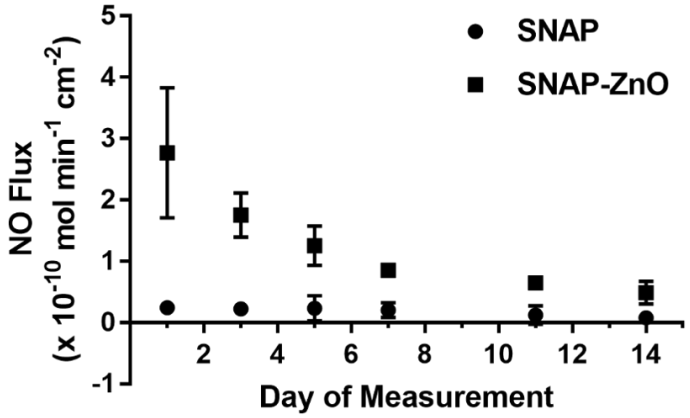

Figure 2.3. NO release profile for SNAP vs. SNAP-ZnO films for 14 days. (n=3)

To confirm that SNAP crystals were blended and ZnO-NPs were present and evenly distributed on the surface of the samples, fabricated films (SNAP-ZnO) were mapped by EDS and analyzed for the uniform presence of zinc and sulfur. The coatings and impregnation of SNAP and ZnO-NPs were found to be uniform as shown in **Figure 2.4 A and B** indicating that the fabrication method had no adverse effect on the stability of SNAP or ZnO-NPs. This uniform distribution is also a good indication that the coating method is reliable to be used for microbial adhesion prevention on the medical device's surface.

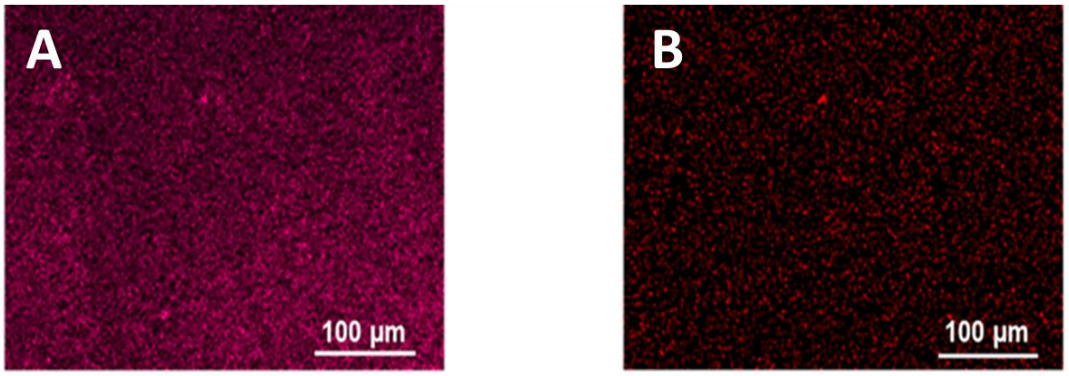

Figure 2.4. Energy dispersive X-ray Spectroscopy images of the elements present in different coatings. A) Sulfur element map for SNAP-ZnO films and B) Zinc element map for SNAP-ZnO films

Analysis of ZnO-NP Leaching

The decomposition of all RSNOs into radical NO and disulfides is facilitated through the homolytic cleavage of the sulfur-nitroso bond which can be accelerated by the administration of certain transition metal ions. The reduction of Cu^{2+} metal ions to Cu^{+} has been thoroughly investigated in its catalytic properties with RSNOs.[39] While the exact mechanism is still being investigated, Zn has previously been reported to display a

similar catalytic effect.[30] The Zn^{2+} mediated reactivity of RSNOs has a more unique proposed mechanism when compared to Cu^{+} as it keeps its ionic state consistent throughout the catalytic process. After RSNO degradation to RS^{-} + NO, residual RS^{-} molecules end up forming disulfide RSSR compounds when in an aqueous environment. Zn is able to form a complex with these residual RS^{-} ions to prevent disulfide bond formation, allowing for possible regeneration of RSH molecules after complete NO release and subsequent renitrosation into its original RSNO form.[40] The presence of these thiols would also assist in the increased NO release of Zn incorporated SNAP films as RSH molecules have been demonstrated to have destabilizing effects to RSNOs.[41]

While Zn has many beneficial effects, and is vital for numerous physiological pathways, it is important that a majority of the ZnO-NP stays within the tested polymer films to help facilitate the catalytic NO release from the blended SNAP. To detect for any ZnO-NP diffusion, ICP-MS was performed on 1 cm^2 measured samples. Only the highest weight percent (10%) of ZnO-NPs was used for all ICP-MS studies to observe any potential leaching into the surrounding environment. After 14 days of soaking in DMEM at 37°C, ZnO films demonstrated only 1.08% of the total Zn leached into solution while SNAP-ZnO films also had a negligible 3.17% leached. This shows how well encapsulated the nanoparticles are within the topcoats of the synthesized CarboSil polymer films and demonstrates the potential longevity of their catalytic activity. As NO is emitted from the polymer into an aqueous environment, trace amounts of nitric acid are formed at the material interface which can increase the potential Zn solubility and account for the slightly higher leachate result. The increase in Zn leaching from the

SNAP-ZnO films could also be assisting in the increased antimicrobial activity, which is described in detail in the next section.

Enhanced Antimicrobial Efficacy and Low Cytotoxicity of NO-Releasing Materials Topcoated with ZnO-NP

Bacterial adhesion is a common challenge faced by medical implants. It is triggered in response to medical devices coming in contact with the fluidic biological milieu provided by the human physiology and the surgical wound provided during the insertion of the medical device. This bacterial adhesion in the first few hours of implantation can lead to infection of the site and further cause medical device failure or even death. Furthermore, *S. aureus* and *P. aeruginosa* are two of the most commonly found nosocomial pathogens. Due to the stated reasons, a bacterial adhesion study was carried out for the fabricated materials for 24 hours using *S. aureus* and *P. aeruginosa*. Another important point to note here is that both bacteria studies were done after an initial 24 hours soaking of the materials in PBS. This step allowed for initial metal-ion and SNAP leachates to be removed from the study and hence prevent any false results due to higher percentage of leachates during bacterial incubation.

Due to the antibacterial properties of NO, active release of NO from the donor molecule incorporated in the hydrophobic polymeric films can reduce the chances of biomedical device related infections or HAIs. The adhesion of bacteria to the NO-releasing material can further be reduced increasing the NO release or having an initial burst release followed by the synergistic bactericidal activity of a metal ion. As seen from **Figure 2.5 A**, in case of *S. aureus*, there is a 78.02 ±25.03% reduction (~0.5 log) when only ZnO-NPs are applied as a topcoat on CarboSil samples. This is due to the

bactericidal properties of ZnO-NPs as mentioned in the introduction. NO-releasing CarboSil (SNAP films) in comparison have a higher killing efficiency at 87.72 ±7.53% (~1 log) reduction due to even better bactericidal properties of diffusion based bacterial cytotoxicity of NO. However, the synergistic effects are clearly seen and very prominent as there is a 99.03 ±0.50% (~2 log) reduction in case of SNAP-ZnO films. This reduction is seen to increase when ZnO-NPs are applied as topcoat to SNAP containing polymer and hence it can be concluded that ZnO-NPs and NO have synergistic bactericidal effects against *S. aureus*. It is also important to note here that in addition to the higher reduction with SNAP-ZnO materials, there was also a high reduction between ZnO vs SNAP-ZnO (95.59 ±2.29%) and SNAP vs SNAP-ZnO (92.11 ±4.10%) materials.

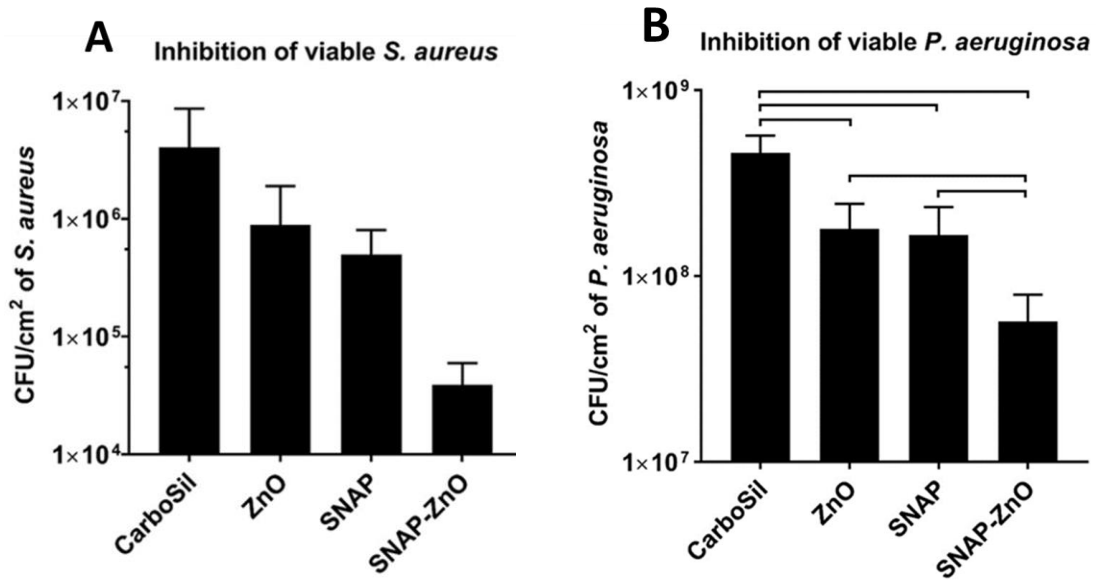

Figure 2.5. Inhibition of viable bacteria adhesion over 24-hour exposure in physiological conditions. **A)** Comparison in adhesion of *S. aureus* between CarboSil, ZnO, SNAP and SNAP-ZnO films. **B)** Comparison in adhesion of *P. aeruginosa* between CarboSil, ZnO, SNAP and SNAP-ZnO films. (All bars indicate statistical significance with $p<0.05$; n=4 for *S. aureus*; n=3 for *P. aeruginosa*)

Similar results were observed in case of *P. aeruginosa* but with a smaller log reduction in all the bactericidal agent containing films (**Figure 2.5 B**). This may be attributed to the extra cell membrane that Gram negative bacteria like *P. aeruginosa* have. A 60.98 ±14.18% (~0.5 log) reduction was seen in ZnO, and a 63.76 ±14.88% reduction for SNAP materials was seen when compared to CarboSil. Although when both the bactericidal agents were combined, SNAP-ZnO materials yielded an 87.63 ±4.86% (~1 log) reduction when compared to CarboSil samples. All of these reductions were significant with a p value<0.05. This higher reduction is seen as a synergistic effect of ZnO-NPs and NO's antimicrobial activity. In addition to these reductions, there was also a high reduction between ZnO vs SNAP-ZnO (65.86 ±13.42%) and SNAP vs SNAP-ZnO (68.29 ±12.46) materials. Thus, from the antimicrobial assays used to test the synergistic combination of ZnO nanoparticles with NO donor, the hybrid materials were able to demonstrate superior infection-resistant properties that can be applied to medical device coatings (**Table 2.4**).

Table 2.4. Reduction of bacteria/cm^2 seen on test samples compared to CarboSil control

	Reduction in *S. aureus* (%)	**Reduction in *P. aeruginosa* (%)**
CarboSil vs ZnO	78.02 ±25.03	60.98 ±14.18
CarboSil vs SNAP	87.72 ±7.53	63.76 ±14.88
CarboSil vs SNAP-ZnO	99.03 ±0.50	87.63 ±4.86
ZnO vs SNAP-ZnO	95.59 ±2.29	65.86 ±13.42
SNAP vs SNAP-ZnO	92.11 ±4.10	68.29 ±12.46

While the material demonstrated controlled NO release and antibacterial efficacy, it was important to validate that the material is not toxic to the mammalian cells. In a real-life scenario, this would mean protecting the host tissue from toxic side effects

during the time of application. The WST-8 dye-based test showed that there was no significant difference in the viability when the CarboSil was compared with cells exposed to leachates from SNAP, ZnO or SNAP-ZnO materials (**Figure 2.6**). This means that the material does not possess any cytotoxicity toward mouse fibroblast cells. This negligible cytotoxicity was expected based from the leaching test results of Zn ions (ICP-MS results) and SNAP and serves as a proof-of-concept for the potential biocompatibility of the material.

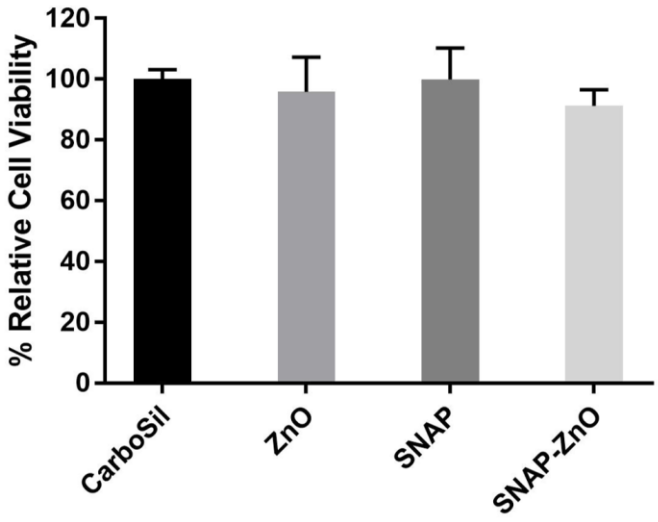

Figure 2.6. Percentage relative cell viability of mouse fibroblast cells after 24-hour exposure to leachates from CarboSil, ZnO, SNAP and SNAP-ZnO films. (n=3).

While the same concentration of SNAP by itself for NO-release has shown negligible cytotoxicity in the past,[42] copper nanoparticles have also assisted NO release from SNAP and demonstrated no toxicity towards mammalian cells.[26] However, this is the first time that similar results have been recorded with the SNAP-ZnO combination. Another advantage of such NO based strategies is that it is highly compatible with other bacteria resistant or bactericidal approaches such as zwitterions, quaternary ammonium

ions, silicone oil, and diatomaceous earth particle.[32,43-45] The non-cytotoxic nature combined with the antibacterial properties offers a potential alternative therapeutic option instead of silver nano particles or antibiotics which have the issue of cytotoxicity or bacterial resistance.

2.4. CONCLUSION

This work demonstrates the potential beneficial effects of ZnO-NPs on the catalytic release and antimicrobial effects of NO under physiological conditions. The hybrid materials, SNAP-ZnO, was composed of a base film (50 mg/ml CarboSil with 10 wt.% SNAP) and a topcoat (2 dips of 25 mg/ml CarboSil solution containing 10wt.% ZnO-NP). The 10 wt.% of ZnO-NPs in SNAP-ZnO samples was able to retain more SNAP molecules within it (7.75 wt.% loss of SNAP) when compared to samples with no (13.85 wt.%), 1 (12.697 wt.%) or 5 (8.821 wt.%) wt.% ZnO-NPs in them. EDS-mapping showed that the hybrid material, SNAP-ZnO, had a uniform distribution of ZnO-NPs and SNAP molecules in it. NO release measurements also demonstrated SNAP-ZnO's ability to maintain physiological levels of NO release for up to 14 days. Antibacterial efficacy at 99.03 ±0.50% and 87.63 ±4.86% reduction for *S. aureus* and *P. aeruginosa*, respectively, were promising results. Finally, low cytotoxicity results demonstrated by SNAP-ZnO samples establish the need to fabricate antibacterial materials that are mammalian cell friendly.

These studies represent preliminary data that can be used to design a long-term antimicrobial and biocompatible device coating that has high potential for use in different implantable materials. In the future, more similar mammalian cell friendly metal-ions that

can be combined with nitric oxide donors to tune NO release for biomedical purposes can be designed for longer term use that can be tested with *in vivo* conditions.

2.5 REFERENCES

1. von Eiff C, Jansen B, Kohnen W, Becker K. Infections associated with medical devices: pathogenesis, management and prophylaxis. Drugs 2005;65(2):179-214.

2. Harding JL, Reynolds MM. Combating medical device fouling. Trends Biotechnol 2014;32(3):140-6.

3. Prevention CfDCa. Healthcare-Associated Infections.

4. Donlan RM. Biofilms and device-associated infections. Emerging Infectious Diseases 2001;7(2):277-281.

5. Singha P, Locklin J, Handa H. A review of the recent advances in antimicrobial coatings for urinary catheters. Acta Biomaterialia 2017;50:20-40.

6. Al-Sa'doni H, Ferro A. S-Nitrosothiols: a class of nitric oxide-donor drugs. Clin Sci (Lond) 2000;98(5):507-20.

7. Al-Sa'doni HH, Khan IY, Poston L, Fisher I, Ferro A. A Novel Family of S-Nitrosothiols: Chemical Synthesis and Biological Actions. Nitric Oxide 2000;4(6):550-560.

8. Nablo BJ, Chen T-Y, Schoenfisch MH. Sol−Gel Derived Nitric-Oxide Releasing Materials that Reduce Bacterial Adhesion. Journal of the American Chemical Society 2001;123(39):9712-9713.

9. Hetrick EM, Schoenfisch MH. Antibacterial nitric oxide-releasing xerogels: Cell viability and parallel plate flow cell adhesion studies. Biomaterials 2007;28(11):1948-1956.

10. Carpenter AW, Schoenfisch MH. Nitric oxide release: part II. Therapeutic applications. Chem Soc Rev 2012;41(10):3742-52.

11. Yang L, Wang X, Suchyta DJ, Schoenfisch MH. Antibacterial Activity of Nitric Oxide-Releasing Hyperbranched Polyamidoamines. Bioconjugate Chemistry 2017.

12. Zhang H, Annich GM, Miskulin J, Stankiewicz K, Osterholzer K, Merz SI, Bartlett RH, Meyerhoff ME. Nitric Oxide-Releasing Fumed Silica Particles: Synthesis, Characterization, and Biomedical Application. Journal of the American Chemical Society 2003;125(17):5015-5024.

13. Reynolds MM, Frost MC, Meyerhoff ME. Nitric Oxide-Releasing Hydrophobic Polymers: Preparation, Characterization, And Potential Biomedical Applications. Free Radical Biology & Medicine 2004;37(7):926-936.

14. Brisbois EJ, Handa H, Major TC, Bartlett RH, Meyerhoff ME. Long-term nitric oxide release and elevated temperature stability with S-nitroso-N-acetylpenicillamine (SNAP)-doped Elast-eon E2As polymer. Biomaterials 2013;34(28):6957-66.

15. Backlund CJ, Worley BV, Schoenfisch MH. Anti-biofilm action of nitric oxide-releasing alkyl-modified poly(amidoamine) dendrimers against Streptococcus mutans. Acta Biomaterialia.

16. Cai W, Wu J, Xi C, Meyerhoff ME. Diazeniumdiolate-doped poly(lactic-co-glycolic acid)-based nitric oxide releasing films as antibiofilm coatings. Biomaterials 2012;33(32):7933-7944.

17. Handa H, Meyerhoff ME, Bartlett RH, Brisbois EJ, Refahiyat L. Sustained nitric oxide release coating using diazeniumdiolate-doped polymer matrix with ester capped poly (lactic-co-glycolic acid) additive. US Patent App. 14/430,545; 2013.

18. Askew SC, Butler AR, Flitney FW, Kemp GD, Megson IL. Chemical mechanisms underlying the vasodilator and platelet anti-aggregating properties of S-nitroso-N-acetyl-dl-penicillamine and S-nitrosoglutathione. Bioorganic & Medicinal Chemistry 1995;3(1):1-9.

19. Singh SP, Wishnok JS, Keshive M, Deen WM, Tannenbaum SR. The chemistry of the S-nitrosoglutathione/glutathione system. Proceedings of the National Academy of Sciences 1996;93(25):14428-14433.

20. Hogg N. THE BIOCHEMISTRY AND PHYSIOLOGY OF S-NITROSOTHIOLS. Annual Review of Pharmacology and Toxicology 2002;42(1):585-600.

21. Goudie MJ, Brisbois EJ, Pant J, Thompson A, Potkay JA, Handa H. Characterization of an S-nitroso-N-acetylpenicillamine–based nitric oxide releasing polymer from a translational perspective. International Journal of Polymeric Materials and Polymeric Biomaterials 2016;65(15):769-778.

22. Ning C, Wang X, Li L, Zhu Y, Li M, Yu P, Zhou L, Zhou Z, Chen J, Tan G and others. Concentration Ranges of Antibacterial Cations for Showing the Highest Antibacterial Efficacy but the Least Cytotoxicity against Mammalian Cells: Implications for a New Antibacterial Mechanism. Chemical research in toxicology 2015;28(9):1815-1822.

23. Yakoob J, Abbas Z, Usman MW, Awan S, Naz S, Jafri F, Hamid S, Jafri W. Comparison of Antimicrobial Activity of Zinc Chloride and Bismuth Subsalicylate Against Clinical Isolates of Helicobacter pylori. Microbial Drug Resistance 2013;20(4):305-309.

24. Reddy KM, Feris K, Bell J, Wingett DG, Hanley C, Punnoose A. Selective toxicity of zinc oxide nanoparticles to prokaryotic and eukaryotic systems. Applied Physics Letters 2007;90(21):213902.

25. Choi E-K, Lee H-H, Kang M-S, Kim B-G, Lim H-S, Kim S-M, Kang I-C. Potentiation of bacterial killing activity of zinc chloride by pyrrolidine dithiocarbamate. The Journal of Microbiology 2010;48(1):40-43.

26. Pant J, Goudie MJ, Hopkins SP, Brisbois EJ, Handa H. Tunable Nitric Oxide Release from S-Nitroso-N-acetylpenicillamine via Catalytic Copper Nanoparticles

for Biomedical Applications. ACS Applied Materials & Interfaces 2017;9(18):15254-15264.

27. Wonoputri V, Gunawan C, Liu S, Barraud N, Yee LH, Lim M, Amal R. Copper Complex in Poly(vinyl chloride) as a Nitric Oxide-Generating Catalyst for the Control of Nitrifying Bacterial Biofilms. ACS Applied Materials & Interfaces 2015;7(40):22148-22156.

28. Wonoputri V, Gunawan C, Liu S, Barraud N, Yee LH, Lim M, Amal R. Iron Complex Facilitated Copper Redox Cycling for Nitric Oxide Generation as Nontoxic Nitrifying Biofilm Inhibitor. ACS Applied Materials & Interfaces 2016;8(44):30502-30510.

29. Harding JL, Reynolds MM. Composite materials with embedded metal organic framework catalysts for nitric oxide release from bioavailable S-nitrosothiols. Journal of Materials Chemistry B 2014;2(17):2530-2536.

30. McCarthy CW, Guillory RJ, Goldman J, Frost MC. Transition-Metal-Mediated Release of Nitric Oxide (No) from S-Nitroso-N-Acetyl-D-Penicillamine (SNAP): Potential Applications for Endogenous Release of No at the Surface of Stents Via Corrosion Products. ACS applied materials & interfaces 2016;8(16):10128-10135.

31. Singha P, Pant J, Goudie MJ, Workman CD, Handa H. Enhanced antibacterial efficacy of nitric oxide releasing thermoplastic polyurethanes with antifouling hydrophilic topcoats. Biomaterials Science 2017.

32. Liu Q, Singha P, Handa H, Locklin J. Covalent Grafting of Antifouling Phosphorylcholine-Based Copolymers with Antimicrobial Nitric Oxide Releasing Polymers to Enhance Infection-Resistant Properties of Medical Device Coatings. Langmuir 2017.

33. Cha KH, Meyerhoff ME. Compatibility of Nitric Oxide Release with Implantable Enzymatic Glucose Sensors Based on Osmium (III/II) Mediated Electrochemistry. ACS Sensors 2017;2(9):1262-1266.

34. Vanhoe H, Vandecasteele C, Versieck J, Dams R. Determination of iron, cobalt, copper, zinc, rubidium, molybdenum, and cesium in human serum by inductively coupled plasma mass spectrometry. Analytical Chemistry 1989;61(17):1851-1857.

35. Kark RP, Poskanzer DC, Bullock JD, Boylen G. Mercury poisoning and its treatment with N-acetyl-D, L-penicillamine. New England Journal of Medicine 1971;285(1):10-16.

36. Wo Y, Li Z, Colletta A, Wu J, Xi C, Matzger AJ, Brisbois EJ, Bartlett RH, Meyerhoff ME. Study of crystal formation and nitric oxide (NO) release mechanism from S-nitroso-N-acetylpenicillamine (SNAP)-doped CarboSil polymer composites for potential antimicrobial applications. Composites Part B: Engineering 2017.

37. Wo Y, Li Z, Brisbois EJ, Colletta A, Wu J, Major TC, Xi C, Bartlett RH, Matzger AJ, Meyerhoff ME. Origin of long-term storage stability and nitric oxide release behavior of carbosil polymer doped with S-nitroso-N-acetyl-D-penicillamine. ACS applied materials & interfaces 2015;7(40):22218-22227.

38. Sundaram J, Pant J, Goudie MJ, Mani S, Handa H. Antimicrobial and physicochemical characterization of biodegradable, nitric oxide-releasing nanocellulose–chitosan packaging membranes. Journal of agricultural and food chemistry 2016;64(25):5260-5266.

39. Williams DLH. The chemistry of S-nitrosothiols. Accounts of chemical research 1999;32(10):869-876.

40. Kozhukh J, Lippard SJ. Zinc Thiolate Reactivity toward Nitrogen Oxides: Insights into the Interaction of Zn2+ with S-Nitrosothiols and Implications for Nitric Oxide Synthase. Inorganic chemistry 2012;51(13):7346-7353.

41. Singh RJ, Hogg N, Joseph J, Kalyanaraman B. Mechanism of Nitric Oxide Release from S-Nitrosothiols. Journal of Biological Chemistry 1996;271(31):18596-18603.

42. Pant J, Goudie MJ, Chaji SM, Johnson BW, Handa H. Nitric oxide releasing vascular catheters for eradicating bacterial infection. Journal of Biomedical Materials Research Part B: Applied Biomaterials;0(0).

43. Pant J, Gao J, Goudie MJ, Hopkins SP, Locklin J, Handa H. A multi-defense strategy: Enhancing bactericidal activity of a medical grade polymer with a nitric oxide donor and surface-immobilized quaternary ammonium compound. Acta Biomaterialia 2017;58(Supplement C):421-431.

44. Goudie MJ, Pant J, Handa H. Liquid-infused nitric oxide-releasing (LINORel) silicone for decreased fouling, thrombosis, and infection of medical devices. Scientific Reports 2017;7(1):13623.

45. Grommersch B, Pant J, Hopkins SP, Goudie MJ, Handa H. Bio-Templated Synthesis and Characterization of Mesoporous Nitric Oxide-Releasing Diatomaceous Earth Silica Particles. ACS Applied Materials & Interfaces 2017.

CHAPTER 3

COVALENTLY BOUND S-NITROSO-N-ACETYLPENICILLAMINE TO ELECTROSPUN POLYACRYLONITRILE NANOFIBERS FOR MULTIFUNCTIONAL TOPICAL HEALING APPLICATIONS[2]

[2] Christina D. Workman, Sean Hopkins, Jitendra Pant, Marcus Goudie, Hitesh Handa. To be submitted to *Journal of Materials Chemistry B.*

ABSTRACT

Attachment of a nitric oxide (NO) donor to an electrospun polymer has the potential to prolong the wound-healing actions of the material. This study presents the novel, covalent attachment of *S*-nitroso-*N*-acetylpenicillamine (SNAP) to polyacrylonitrile (PAN) fibers. By attaching the NO donor to the polymer, rather than blending it, leaching is reduced to maintain a NO flux within the physiologically relevant range for a longer duration. The synthesized fibers were characterized using a variety of techniques such as SEM, ^{1}H NMR, and drop shape analysis. Due to NO's potent antimicrobial activity, the SNAP-PAN fibers demonstrated a 2-log reduction of *S. aureus* adhesion. Furthermore, the extended zone of inhibition of *S. aureus* by SNAP-PAN demonstrates the ability of NO to impact the environment surrounding the material, in addition to the environment in direct contact. The NO content of this material, the hydrophilicity of PAN, and the fibrous network led to an increased fibroblast proliferation and attachment, an important event for wound closure. The results from this study demonstrate a novel preparation and design of NO-releasing fibers to provide multiple benefits for chronic and acute wound healing applications.

3.1 INTRODUCTION

Chronic wounds affect an estimated 6.5 million patients in the United States alone, resulting in nearly $25 billion spent on treatment annually [1,2]. Chronic wounds are often distinguished by their inability to heal within three months and are accompanied by persistent inflammation, pain and infection. These wounds are typically marked by a decline in quality of life and the use of significant healthcare resources. Chronic wounds, such as diabetic ulcers and pressure sores, are on the rise as the population ages, leaving many with a heavy financial burden and poor healing outcomes. In 2005, it was estimated that the prevalence of pressure sores was between 1.3 and 3 million in the United States alone [3]. This has led to a high demand for a wound dressing that can positively impact the inflammatory, proliferative and remodeling stages of the healing process, while also providing a protective barrier.

In recent years, electrospinning polymer scaffolds have become a popular focus for wound dressing applications due to their high porosity and ability to remove exudates from a wound, while allowing for oxygen diffusion to promote healing [4,5]. Electrospun nanofibers are also the ideal scaffold to use for cell migration and attachment due to its ability to mimic the size of native extracellular matrix (ECM). This allows the mesh network of the nanofibers to provide scaffolding for fibroblasts for the re-epithelialization of the wound area [6,7]. One particular polymer, polyacrylonitrile (PAN), has demonstrated excellent fibroblast seeding owing to its moderate wettability [7]. PAN nanofibers are relatively simple to fabricate with low production costs overall, making it a viable option for wound dressing designs. PAN-based fibers have been used in a wide range of applications such as filtration membranes and textiles. More recently, PAN fibers have

been modified with metal ions, such as silver, for antimicrobial biomaterials [8]. While these fibers were successful in antibacterial experiments, there have been some concerns with the cytotoxicity of metal ions [9]. Overall, the versatility and ease of electrospinning of PAN made it an ideal selection for our material in this study.

Perhaps the biggest concern in the management of wounds is the prevention of infection. An open wound is an entryway for a variety of bacteria, especially for the opportunistic microflora that normally reside on the skin. With the emergence of antibiotic resistant bacteria, namely methicillin-resistant *S. aureus* (MRSA), new approaches for treatment and prevention are an urgent need. MRSA is frequently contracted in healthcare settings and is reported to cause over 11,000 deaths in the United States each year [10,11]. The current treatment option for MRSA is vancomycin, deemed the gold standard in treating resistant pathogens. The extensive use of this antibiotic has now lead to an emergence of vancomycin-resistant *S. aureus* (VRSA) and vancomycin-resistant *enterococcus* (VRE) causing the death rate to rise [12,13]. This precipitates a growing alarm for researchers and healthcare providers worldwide.

To address the need for new antimicrobial agents, research has turned to nitric oxide (NO), the endothelium-derived relaxation factor identified by Furchgott, Ignarro, and Murad in 1987 [14,15]. NO has been a popular molecule to administer as a targeted and localized therapeutic agent due to its role in important physiological functions in vasculature, such as platelet deactivation, vasodilation, and angiogenesis [14,16]. An additional mechanism seen with NO is through its ability to exhibit biocidal activity against foreign pathogens, such as bacteria, protozoa, and viruses mainly through

peroxynitrite formation and nitrosative stress that alters protein function [17,18]. These attributes have prompted many research groups to develop NO donor molecules and fabricate polymeric materials that release NO [19]. Extensive research has surrounded *S*-nitrosothiols as synthetic donors, as they have demonstrated potent pharmaceutical and physiological functions [20,21]. While the results have been promising, the duration of NO release comparable to physiological levels (surface flux of 0.5-4x10^{-10} mol cm^{-2} min^{-1}) is limited due to the leaching of NO donor compounds from the material [22]. To circumvent this issue, we propose a novel method of covalent attachment of the *S*-nitrosothiol, *S*-nitroso-*N*-acetyl-penicillamine (SNAP), to an electrospun PAN fiber scaffold to reduce leaching of the antimicrobial, promote better wound healing, and reduce the risk of infection.

3.2 MATERIALS AND METHODS

Materials

Polyacrylonitrile (PAN), *N*-acetyl-*D*-penicillamine (NAP), sodium nitrite ($NaNO_2$), concentrated sulfuric acid (H_2SO_4), pyridine, acetic anhydride, hexanes, anhydrous magnesium sulfate, t-butyl nitrite, cyclam (1,4,8,11-tetraazacyclotetradecane), ethylene diamine (EDA), sodium acetate, Ellman's reagent (5,5'-dithiobis-(2-nitrobenzoic acid))(DTNB), phosphate buffer saline (PBS), ethylenediamine tetraacetic acid (EDTA), and DAPI (4',6-Diamidino-2-Phenylindole, Dihydrochloride) were acquired from Sigma Aldrich (St. Louis, MO). Concentrated hydrochloric acid (HCl), Alexa Flour 488 Phalloidin, and methanol were purchased from Fisher Scientific (Hampton, NH). Gram positive *Staphylococcus aureus* (ATCC 6538, *S.aureus*) and 3T3 mouse fibroblast (ATCC-1658) were obtained from American Type Culture Collection

(Manassas, VA). Milli-Q filter was used to synthesize deionized (DI) water for all aqueous solutions. Miller and Luria Broth (LB), Lennox and Luria Agar (LA) were purchased from Fischer BioReagents (Fair Lawn, NJ).

Synthesis of *S*-nitroso-*N*-acetyl-penicillamine (SNAP)

SNAP was synthesized according to a previously reported protocol with slight modifications [23]. In short, an equimolar ratio of NAP and $NaNO_2$ were added to a beaker containing a 1:1 mixture of water and methanol with 2M H_2SO_4 and 2M HCl. The mixture was allowed to stir and cool, followed by submersion of the beaker in an ice bath to facilitate precipitation of SNAP crystals. After several hours the crystals were collected via vacuum filtration and dried for 24 hours. During the entire duration of the experiment the solution and crystals were shielded from light.

Synthesis of *N*-acetyl-*D*-penicillamine thiolactone (NAP-thiolactone)

NAP thiolactone was synthesized following a previously described method.[24] Briefly, 5g of NAP was dissolved in 10 mL pyridine and chilled over ice. In a separate vial, 10 ml of pyridine and 10 mL of acetic anhydride were combined and chilled. Once each solution reached 0°C they were slowly combined and stirred for 24 h. The resulting light pink solution was evaporated at 45°C and slowly increased to 60°C to remove the pyridine. The remaining product was dissolved in 20 mL of chloroform and washed with hydrochloric acid (HCl) using a separatory funnel to isolate the organic layer. The washing step was repeated and the collected organic layer was dried with magnesium sulfate. The magnesium sulfate was then filtered off via vacuum filtration and the liquid collected was evaporated at room temperature to remove the chloroform. The solid

collected was washed with hexanes and vacuum filtered to collect the final crystalline product.

Modification of Polyacrylonitrile (PAN) for SNAP Attachment

In order to attach the SNAP molecule to PAN's polymer chain, first the PAN molecule had to be functionalized with an amine group. This required a reaction between the cyanide groups on the PAN chain and EDA. First, 1g of PAN was suspended in ethanol with a 10-fold excess of EDA and refluxed at 70°C for 12 h. Argon gas was used to continuously purge the reaction flask. After 12 h the solid was collected via vacuum filtration and washed with DI water and ethanol. The dried aminated PAN was re-dissolved in DMF to achieve a 12 wt % solution. NAP thiolactone was next added to the solution at a 1:1 molar ratio to the amine groups, allowing for a ring opening reductive amination of the primary amine group. The solution was allowed to stir for 24 h to ensure completion of the reaction. Lastly, t-butyl nitrite was used to nitrosate the thiol groups. The t-butyl was first chelated of any copper stabilizers using a 20 mM cyclam solution before being added to the NAP functionalized with PAN. The complete reaction scheme can be seen in **Figure 3.1**.

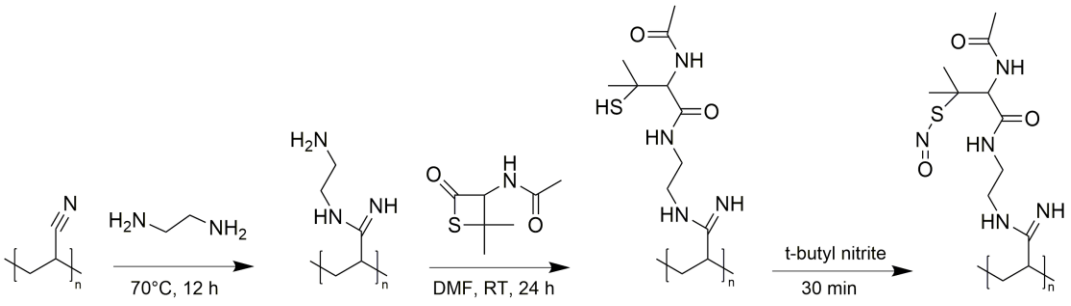

Figure 3.1. Schematic for the covalent attachment of SNAP to the PAN polymer chain.

Electrospinning of SNAP-PAN fibers

Fabrication of SNAP-PAN fibers were done using a 12 wt% solution of polymer in DMF. The nitrosation of the polymer solution was done immediately before electrospinning. Plastic syringes (10 mL) fitted with a blunt, 1" 18G needle were placed onto a syringe pump with the nitrosated polymer solution (Razel Scientific Instruments, St. Albans, VT). A high voltage power supply (Gamma High Voltage, Ormond Beach, FL) was used to supply 14 kV to the needle while a grounded collector was placed 15 cm away from the tip. Flow rate of the SNAP-PAN solution was optimized and maintained at 1.30 mL h^{-1}. After electrospinning, the fibrous SNAP-PAN scaffolds were dried under vacuum at room temperature for 24 h before being used for any procedures.

Characterization of SNAP-PAN fibers

Amine Quantification

Quantification of EDA attachment to the backbone of PAN was done via a fluorescent ATTO-TAG FQ assay [25]. Fluorescent detection was done using a 96-well plate reader (plate reader) and quantification of primary amine sites was determined using glycine as a reference. The conjugate that forms is maximally excited at 480 nm with an emission of 590 nm.

Thiol Quantification

After NAP-thiolactone attachment, detection of free thiols was done using Ellman's assay [26]. Exposed thiol groups from the covalently attached NAP bind to 5,5'-dithiobis (2-nitrobenzoic acid) (DNTB) and release a dye in solution

measurable at 412 nm. A calibration curve using acetyl cysteine was used as a reference to quantify the NAP attachment.

Nitric oxide (NO) Capacity Quantification

Nitrosated SNAP-PAN films were left to dry under vacuum for 24 h before being tested for NO release. The bound NO on the SNAP-PAN was then catalytically released by placing it into a solution containing 30 µL of 50 mM $CuCl_2$, 1.5 µL of 10 mM cysteine, and 2945 µL of PBS. The total NO was then quantified via chemiluminescence from a Nitric Oxide Analyzer (NOA) (Sievers 280i, GE Analytics, Bounder, CO), where NO is measured from the SNAP-PAN in real time. Once the NO release was exhausted, the resulting NO release curve was integrated and quantified.

NMR analysis

^{1}H NMR was performed on modified PAN samples using a 300 MHz Varian/Agilent mercury spectrometer. Deuterated N,N-dimethylformamide (DMF-d7) was the solvent used for all analysis. Mnova software was used for calculating peak data.

SEM Imaging

Fiber size and mat porosity were examined under a scanning electron microscope (SEM) (FEI Inspect F FEG-SEM). The fiber mats were mounted on a metal stub with double-sided carbon tape and sputter coated with 10 nm gold-palladium using a Leica EM ACE200 sputter coater. Images were taken at accelerating voltage 5 kV.

Static Contact Angle

The static contact angles for the proposed material and the control were measured using a Krüss DSA100 Drop Shape Analyzer via a sessile drop method with DI water. SNAP-PAN films and PAN only films were made via a solvent evaporation method, resulting in a solid film. This study was used to assess if the modification of PAN altered the hydrophilicity of the material.

NO Release Measurements

NO release was quantified using a NO chemiluminescence analyzer (Sievers 280i, GE Analytics, Boulder, CO). NO release readings were recorded at time points of 0, 6, 24, and 48 h. Samples of SNAP-PAN fibers and SNAP blended fibers were wrapped in a dampened Kimwipe and suspended in a humid sample holder to simulate physiological conditions. The humid environment was created by placing a small amount of PBS (with EDTA) in the bottom of the sample holder and warming to 37°C. The NO released was swept and purged by high purity nitrogen gas supplied into the sample holder via the sweep and bubble flows. Oxygen in the reaction chamber produces ozone for the reaction with the released NO, producing a voltage signal in the chemiluminescence detection chamber. The signal was then converted to a concentration and displayed as ppb. Using the NO constant (mol ppb^{-1} s^{-1}), the ppb data was normalized and converted to a NO flux ($x10^{-10}$ mol $mg^{-1}min^{-1}$) in terms of the weight of each sample.

Fibroblast Cell Attachment and Proliferation

Mammalian Cell Culture

A cryopreserved vial containing fibroblast cells was thawed rapidly at room temperature and added to 5 ml of pre-warmed DMEM medium. The cells in the medium were centrifuged at 1100 rpm for 7 minutes. The supernatant was discarded and fresh DMEM medium was added. The cells were then transferred to a sterile 25 cm^2 T-flask and incubated in a humidified incubator with 5% CO_2 at 37°C. DMEM was changed on alternate days to fulfill the nutrients requirements of the cells and were allowed to grow until they became 80-90 % confluent. Thereafter the monolayer of the cells was detached using 0.18% trypsin with 5mM EDTA. The cell count was taken using 0.4% trypan blue dye in a hemocytometer counter.

Imaging

Mouse fibroblast cells were directly cultured onto control PAN and SNAP-PAN fibrous scaffolds to observe cell growth and attachment potential. Fibers were directly electrospun onto 1 cm diameter glass cover slips and placed into a 6 well plate, which were UV sterilized for 30 minutes before testing. Cell cultures containing 500 cells mL^{-1} were then seeded directly to the nanofibers and allowed to incubate for 24 h. The cell nuclei were then stained with DAPI (4',6-diamidino-2-phenylindole) and cytoskeletal structure was observed using Alexa Fluor 488 Phalloidin. Briefly, the cells within the fibrous scaffolds were first fixed in 0.01M PBS containing 5% paraformaldehyde. Alexa Fluor 488 Phalloidin was diluted (1:500 in PBS) and was then administered for 20 minutes followed by

DAPI (300 nM in PBS) for 3 minutes while being protected from light. Finally, cell growth and attachment of the fibroblasts was observed under a fluorescent microscope (EVOS XL, Thermo Fisher Scientific, Waltham, MA).

Evaluation of Antimicrobial Activity

Zone of Inhibition Analysis

A modified, standard agar diffusion assay was conducted to evaluate SNAP-PAN's ability to inhibit bacteria growth via the diffusion of gaseous nitric oxide to the surrounding environment. LB agar plates were inoculated with *S. aureus* (1×10^7 CFU/mL) and spread to cover the entire plate. Circular films with a surface area of 1 cm^2 were placed on the surface on the cultured bacteria. Films of PAN only fibers and SNAP-PAN fibers were compared. Plates were incubated overnight at 37°C. Antimicrobial activity was determined by measuring the diameter of the zones of inhibition. The assay was performed in triplicate to ensure reproducibility.

Quantification of Viable Bacteria Adhesion

In this study, the SNAP-PAN fibers were tested to evaluate the ability for the material to kill and prevent bacteria from adhering to the fiber network. We tested our material against *S. aureus*, a common Gram-positive bacterium acquired in hospital settings. A protocol for quantifying viable CFUs was followed with slight adjustments. In summary, *S. aureus* was grown over night in Luria Broth for 14 h at 37°C while rotating at 150 rpm. The optical density (OD) was measured using a UV-Vis spectrophotometer at 600nm wavelength to

confirm bacteria were in log phase of growth. The solution was centrifuged at 2500 rpm for 7 min and the resulting pellet was collected. The bacteria were re-suspended in sterilized PBS and the OD_{600} adjusted to achieve a CFU/mL in the range of 10^7-10^9 based on a calibration curve for *S. aureus*. Exact weights of SNAP-PAN fibers and SNAP blended fibers were recorded and maintained around 0.70 mg each. Triplicates of each sample type were tested. Samples were incubated in a 24-well plate and exposed to 1 mL of the adjusted bacteria solution. The 24-well plate was incubated on a shaker for 24 hours to allow for interaction between the bacteria and the material. Samples were removed from the solution and gently rinsed with sterilized PBS to remove loosely bound bacteria. The fibers were then sonicated using an Omni-tip homogenizer to collect the bound bacteria in a 1 mL PBS solution. The collected bacteria was serially diluted and spread on LB agar plates. Plates were inverted and incubated overnight at 37°C. The CFUs were then counted and adjusted using the dilution factor to quantify the number of adhered bacteria. Data was reported in terms of CFUs/mg.

$$\% \text{ Bacterial inhibition} = \frac{C_c - C_s}{C_c} \times 100$$

$$C_c - \frac{CFU}{cm^2} \; of \; control \; samples$$

$$C_s - \frac{CFU}{cm^2} \; of \; test \; samples$$

Statistical Analysis

All data are expressed as a mean standard deviation. Results between the test fibers and control fibers were compared and analyzed using a Student's *t*-test. P values were obtained to analyze significance of results.

3.3 RESULTS AND DISCUSSION

Evaluation of SNAP-PAN Fibers

The principal goal for this material was to develop a nanofibrous support with sustained levels of NO release that could be applied for wound healing and tissue scaffold applications. One of the key concerns with NO releasing fibers is how quickly their NO reservoir can be exhausted. Due to the high surface area of dressings formed from nanofibers, blended NO donors will leach at a high rate, which usually exhausts the NO release within the first 24 h. By covalently attaching the NO donor to the backbone of the electrospun polymer, this leaching issue could potentially be circumvented. Before electrospinning of the SNAP functionalized fibers could proceed, a thorough characterization of the modified polymer was first performed. The initial amination step of the cyanide backbone groups on PAN has been previously optimized [27]. Since a difunctional amine reagent was used to modify the PAN, the reaction conditions are extremely sensitive as reacting too long can cause crosslinking between polymer chains and too short of a time would result in low amination functionality. Once the degree of primary amine groups was quantified, the ring opening reaction with NAP-thiolactone and proceeding nitrosation allowed for the covalent attachment of SNAP. Each reaction step was monitored with NMR, which is shown in **Figure 3.2**. Total quantification of amine, NAP, and SNAP conversion is shown in **Table 3.1**. The low conversion of NAP to SNAP is most likely due to NO loss from the electrospinning process.

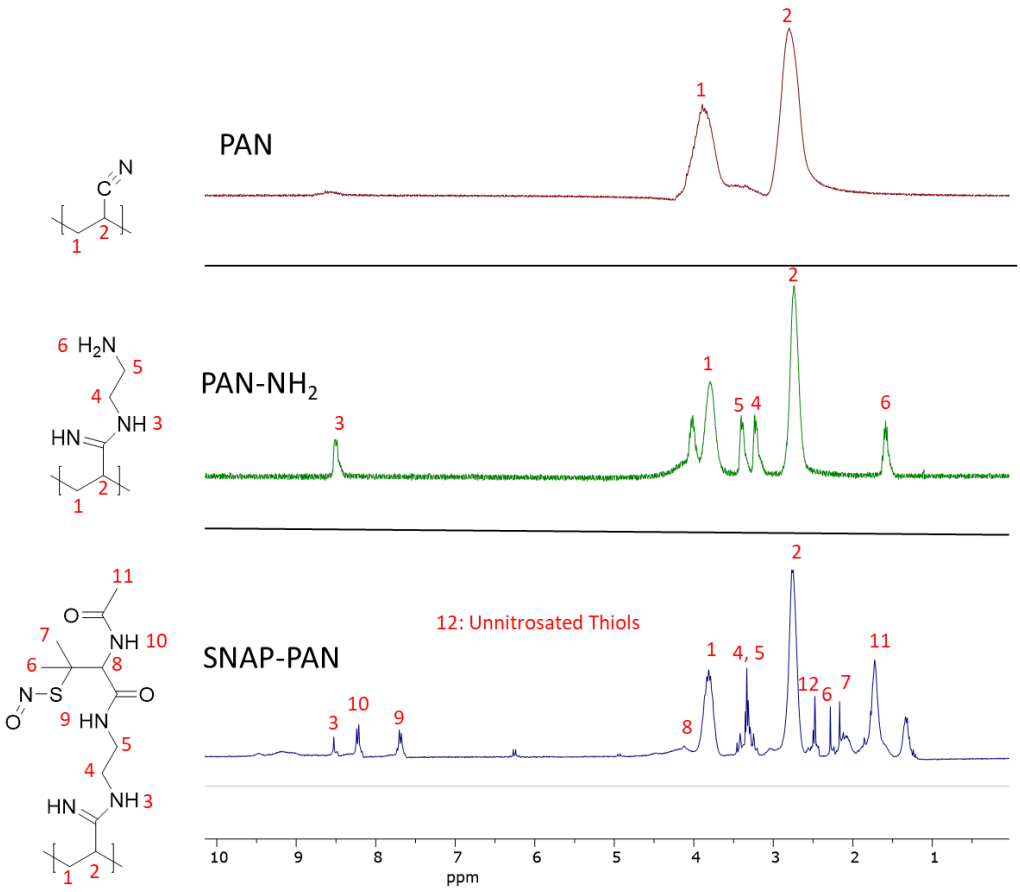

Figure 3.2. The technique of NMR spectroscopy was used to confirm the attachment of the diamine and subsequent attachment of NAP thiolactone.

Table 3.1. Amine/thiol/NO quantification of PAN Fibers

Functionalization of SNAP-PAN Fibers				
	Total Amines (µmol/mg)	Free Thiols (µmol/mg)	Total NO Loaded (µmol/mg)	Conversion Thiol to NO
SNAP-PAN Fibers	2.94 ± 0.07	2.69 ± 0.27	1.02 ±0.05	38%

The synthesized SNAP-PAN was dissolved in DMF at 12 wt% and fibers were electrospun using an applied voltage of 15 kV, 15 cm away from the target, at a rate of

1.30 mL hr^{-1}. One complication that occurred during the electrospinning process was the fibers precipitating immediately from the needle tip before hitting the target. This was due to the t-butyl nitrite still present in the solution after the nitrosation step. To prevent this, SNAP-PAN solutions were allowed to stir uncovered for several hours before electrospinning to evaporate any unreacted t-butyl nitrite and t-butyl alcohol byproduct that formed.

The SEM images of the electrospun fibers are shown in **Figure 3.3** which were used to calculate the average fiber diameter and porosity of PAN and SNAP-PAN. The average diameter was calculated using ImageJ software and was found to be 350 ± 104 nm for PAN and 482 ± 117 nm for SNAP-PAN. Porosity and fiber diameter are important factors when relating to cell migration, adhesion, and even the regulation of proinflammatory macrophages [28-30]. When designing a wound dressing, these parameters should be optimized to maximize the effectiveness.

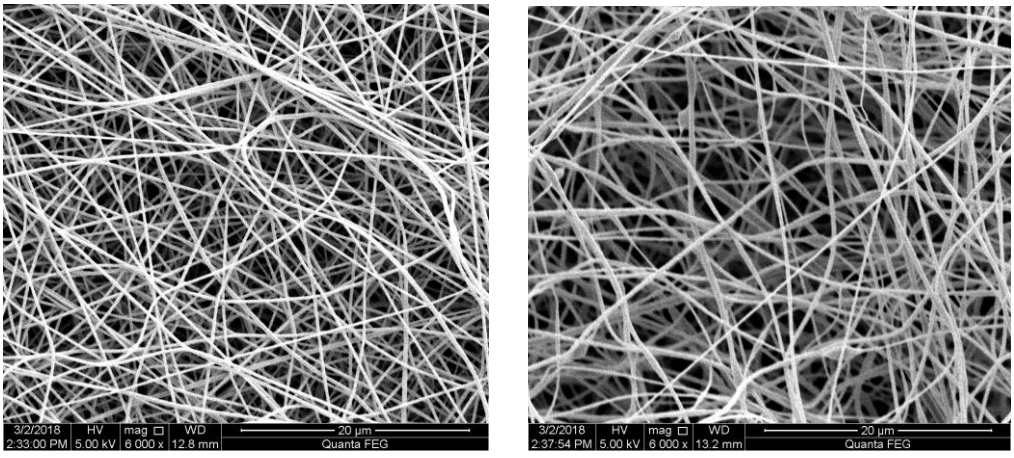

Figure 3.3. SEM images of PAN fibers (left) and SNAP-PAN fibers (right) at a magnification of 6,000x and a voltage of 5 kV.

The static contact angle was measured to determine the hydrophilicity of the PAN material before and after modification with SNAP. Sessile drops of deionized water were applied to solid PAN films and SNAP-PAN fibers to obtain observable drops. We were unable to use fibers due to the rapid absorption of water into the fibrous network. By attaching SNAP to the PAN polymer, there was a notable decrease in the contact angle from 69.77° ± 9.26 to 46.45° ± 3.66 representing an increased hydrophilic nature of the SNAP-PAN material. This indicates that our material will have enhanced wettability, which allows for better fibroblast attachment [31].

Nitric Oxide Release Behavior from Fibers

The NO release from all film types was initiated upon exposure to a dampen Kimwipe and suspension into the humid NOA cell, containing PBS adjusted to a pH of 7.4. These conditions allowed for the homolytic cleavage of the S-N bond on the *S*-nitrosothiol molecule, giving off NO as a free radical [32]. The detection of NO using chemiluminescence is the "gold standard" in quantifying NO release due to its selectivity for the gaseous NO released, rather than the nitrates and nitrites that may also be present. **Figure 3.4** illustrates the enhanced NO release from the PAN fibers with SNAP covalently attached. By directly attaching the SNAP molecule to the polymer chain, rather than blending it, the level of NO release remained in the physiologically relevant range for a longer duration. The SNAP-PAN fibers reached a peak NO flux at 1.38 ± 0.2 (x 10^{-10} mol min^{-1} mg^{-1}) initially and maintained a flux above 0.60 ± 0.067 (x 10^{-10} mol min^{-1} mg^{-1}) after 6 hours of incubation. This is a significant improvement in release duration when compared to previous NO fiber studies that used diazeniumdiolates as the source of NO [33,34]. When evaluating our SNAP-PAN fiber's NO release at 48 hours, it is

important to note that previous studies have evidence suggesting that NO at levels as low as 0.3 (x 10^{-10} mol min^{-1} mg^{-1}) may still have antimicrobial effects [35]. Furthermore, the SNAP blended fibers, with a matched NO concentration to the attached fibers, never exceeded a NO surface flux of 0.06 ± 0.036 (x 10^{-10} mol min^{-1} mg^{-1}) and at 48 hours no release was detected by the NOA. This is most likely a result of the rapid leaching of the SNAP molecule from the fibrous network. The attachment of SNAP to the polymer chain eliminated the concern for leaching of the NO donor, thus sustaining the material's release of the antimicrobial agent. This is the first report of NO-releasing fibers with NO release lasting longer than 24 hours.

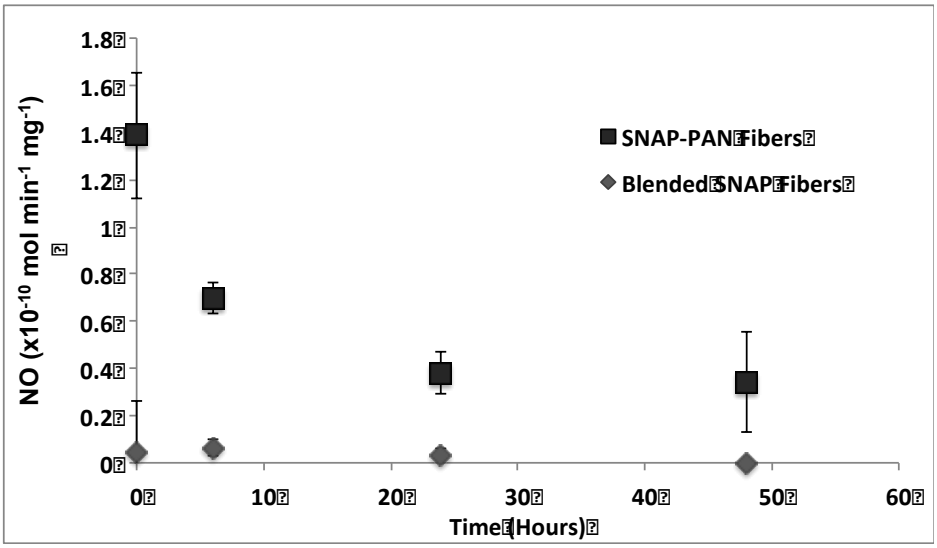

Figure 3.4. The nitric oxide release from SNAP-PAN fibers and SNAP blended fibers is presented as a NO flux. The blended SNAP fibers were completely exhausted of NO after 24 hours.

Support of Cell Attachment and Proliferation

The utilization of modified PAN nanofibers has been used in the past for wound healing scaffold applications and have been demonstrated to support fibroblast growth [5,7,34]. Osteoblasts have also been cultured on porous PAN scaffolds for bone tissue

engineering applications [36]. The combination of NO with polymeric scaffolds specifically has shown to increase the proliferation and attachment of certain cell types such as endothelial cells and fibroblasts while inhibiting others like smooth muscle cells [37,38]. For wound healing specifically, the exogenous release of NO has been shown to significantly increases angiogenesis which ultimately leads to a shorter wound resolution [39]. The proposed study focuses on fibroblast adhesion specifically to SNAP-PAN fibers after 24 h of incubation to further investigate its effectiveness as a topical wound dressing.

The electrospun SNAP-PAN fibers demonstrated a higher amount of growth and attachment when compared to control PAN fibers (**Figure 3.5**). Large aggregations of fibroblasts were seen throughout the SNAP-PAN fibers while the cells attached on control PAN were spread out and lower in overall number. Part of the reason could be due to the increase hydrophilicity of the polymer when functionalized with SNAP, which was shown in an earlier section. The primary reason for this is due to NO's ability to increase the proliferation and activity of fibroblasts [40,41]. Specifically, NO has been shown to increase wound collagen accumulation and consequently improving the overall mechanical strength of the resolved wound area [42]. This accounts for the larger cytoplasmic and nucleic features seen in the fibroblasts cultured on SNAP-PAN when compared to its relative control.

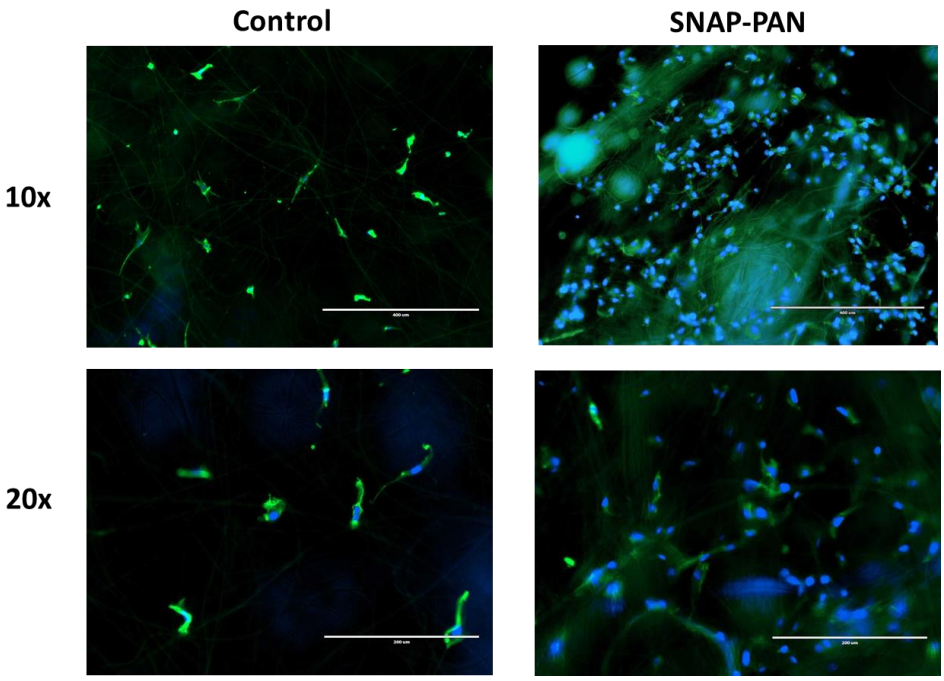

Figure 3.5 Imaging of fibroblasts within the fibrous matrix. Left side: PAN only fibers (control), Right side: SNAP-PAN fibers. Images are at a magnification of 10x and 20x.

Analysis of Antimicrobial Activity

To evaluate the SNAP-PAN material's ability to eliminate bacteria in the surrounding area, the fibers were exposed to *S. aureus* LB agar plates, resulting in zones of inhibition (ZOI) surrounding the material. Zones of inhibition were defined as areas were bacteria growth did not occur. *S. aureus* was selected due to its prevalence in nosocomial infections and the increasing concern of MRSA. As we anticipated, clear zones were observed around the SNAP-PAN fibers resulting from the NO eluded from the SNAP upon warming in the incubator at 37°C, breaking the S-NO bond by thermal decomposition [32]. Due to the innate high surface area of nanofibrous scaffolds, there was a large diffusion of NO to the surrounding agar during the study. The observed zones for SNAP-PAN fibers ranged in size from 14 mm to 18 mm diameters (**Figure 3.6).** It was

also observed that the PAN material alone was not antimicrobial, as no ZOIs existed. This particular study represented the diffusive nature of the NO molecule. This implies that the material will protect the area immediately surrounding the wound in addition to the area in direct contact with the material.

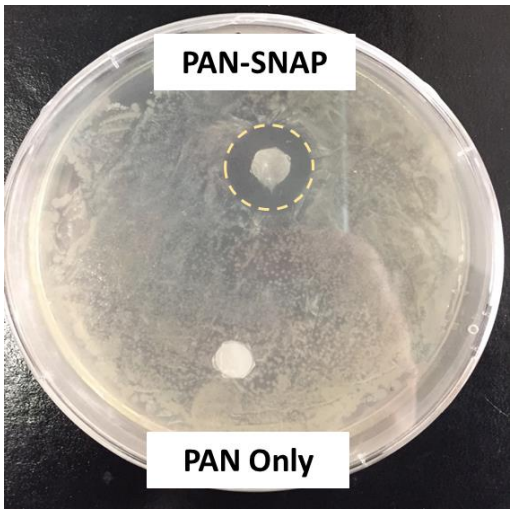

Figure 3.6. Films with a surface area of 1 cm^2 were placed on agar media inoculated with *S. aureus*. PAN-only fibers exhibited no inhibition. Zone of Inhibition is indicated by the dashed lines. SNAP-PAN fibers exhibited an average diameter of 16 ± 2 mm.

The bacteria interaction with the material was further evaluated through an adhesion viability study. Bacteria adhesion to a material's surface leads to biofilm formation, which can be difficult to treat using antibiotics, making it important to prevent initial attachment. Circular films of PAN only and SNAP-PAN fibers were compared for the quantity of viable bacteria adhered within the fiber network. Both fiber types were challenged with *S. aureus* to evaluate their ability to prevent bacteria adhesion. The combination of the hydrophilic polymer and antimicrobial properties of NO led to a 99.71% ($p<0.05$) reduction of viable *S. aureus* (CFU mg^{-1}) on the SNAP-PAN fibers when compared to the PAN-only fibers (**Figure 3.7**). The hydrophilicity of the polymer

allows for the formation of a hydration layer creating a barrier for attachment of bacteria and potentially other contaminants, such as blood proteins [23,43]. The reduction in bacterial growth can be attributed to the NO generation, based on the NO release results we observed. An additional attribute of using NO as an antimicrobial agent in our material is the inability for most bacteria to develop resistance [44]. In summary, the reduced bacterial growth at the site of the wound may allow for more rapid healing and a reduced need for antibiotic treatment.

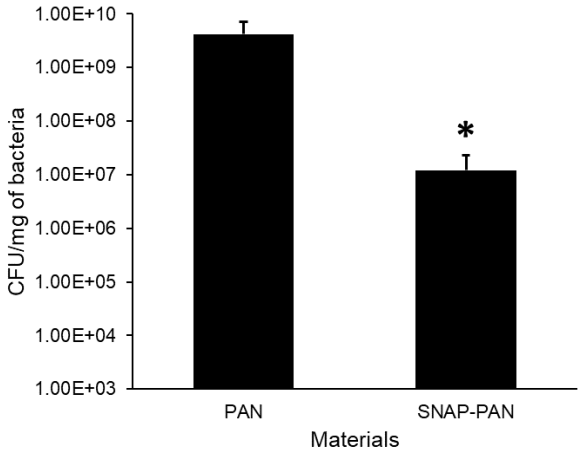

Figure 3.7. Adhered bacteria to the fiber films was quantified using a plate counting method. When compared to the control of PAN-only fibers, the SNAP-PAN fibers had a 99.71% reduction in adhered bacteria. ($p < 0.05$)

3.4. CONCLUSIONS

In this work, a novel wound dressing material demonstrated excellent wound healing and wound protecting properties. Electrospinning the PAN polymer provided a fibrous network for an increased surface area. The high porosity of the fibers provides a network to capture and remove exudate from the wound, while also preventing excessive drying of the wound area. It was also observed that the porous fibers aided in

the epithelialization stage of the wound healing process, acting as a scaffold to support cell attachment and proliferation. By using nitric oxide, a naturally occurring antimicrobial, our material was able to exhibit a 2-log reduction of bacteria growth. The addition of this antimicrobial agent to the polymer scaffold by means of direct attachment allowed for the prolonged usage of the material, reducing the need for reapplication to the wound site. This study provides the initial work towards the development of a novel, multi-functional wound dressing. Future *in vivo* studies will be needed to assess the full synergistic effects of this material.

3.5 REFERENCES

1. Frykberg RG, Banks J. Challenges in the treatment of chronic wounds. *Advances in wound care.* 2015;4(9):560-582.

2. Sen CK, Gordillo GM, Roy S, et al. Human skin wounds: a major and snowballing threat to public health and the economy. *Wound repair and regeneration.* 2009;17(6):763-771.

3. Isenberg JS, Ridnour LA, Espey MG, Wink DA, Roberts DA. Nitric oxide in wound-healing. *Microsurgery: Official Journal of the International Microsurgical Society and the European Federation of Societies for Microsurgery.* 2005;25(5):442-451.

4. Thakur R, Florek C, Kohn J, Michniak B. Electrospun nanofibrous polymeric scaffold with targeted drug release profiles for potential application as wound dressing. *International journal of pharmaceutics.* 2008;364(1):87-93.

5. Liu X, Lin T, Fang J, et al. In vivo wound healing and antibacterial performances of electrospun nanofibre membranes. *Journal of biomedical materials research Part A.* 2010;94(2):499-508.

6. Zahedi P, Rezaeian I, Ranaei-Siadat SO, Jafari SH, Supaphol P. A review on wound dressings with an emphasis on electrospun nanofibrous polymeric bandages. *Polymers for Advanced Technologies.* 2010;21(2):77-95.

7. Groth T, Seifert B, Malsch G, et al. Interaction of human skin fibroblasts with moderate wettable polyacrylonitrile–copolymer membranes. *Journal of Biomedical Materials Research Part A.* 2002;61(2):290-300.

8. Yu D-G, Zhou J, Chatterton NP, Li Y, Huang J, Wang X. Polyacrylonitrile nanofibers coated with silver nanoparticles using a modified coaxial electrospinning process. *International journal of nanomedicine.* 2012;7:5725.

9. Burd A, Kwok CH, Hung SC, et al. A comparative study of the cytotoxicity of silver-based dressings in monolayer cell, tissue explant, and animal models. *Wound repair and regeneration.* 2007;15(1):94-104.

10. Ventola CL. The antibiotic resistance crisis: part 1: causes and threats. *Pharmacy and Therapeutics.* 2015;40(4):277.

11. Klein E, Smith DL, Laxminarayan R. Hospitalizations and deaths caused by methicillin-resistant Staphylococcus aureus, United States, 1999–2005. *Emerging infectious diseases.* 2007;13(12):1840.

12. Levine DP. Vancomycin: understanding its past and preserving its future. *Southern medical journal.* 2008;101(3):284-291.

13. Furuno JP, Perencevich EN, Johnson JA, et al. Methicillin-resistant Staphylococcus aureus and vancomycin-resistant enterococci co-colonization. *Emerging infectious diseases.* 2005;11(10):1539.

14. Carpenter AW, Schoenfisch MH. Nitric oxide release: Part II. Therapeutic applications. *Chemical Society Reviews.* 2012;41(10):3742-3752.

15. Ignarro LJ, Buga GM, Wood KS, Byrns RE, Chaudhuri G. Endothelium-derived relaxing factor produced and released from artery and vein is nitric oxide. *Proceedings of the National Academy of Sciences.* 1987;84(24):9265-9269.

16. Radomski M, Palmer R, Moncada S. Endogenous nitric oxide inhibits human platelet adhesion to vascular endothelium. *The Lancet.* 1987;330(8567):1057-1058.

17. De Groote MA, Fang FC. NO inhibitions: antimicrobial properties of nitric oxide. *Clinical Infectious Diseases.* 1995;21(Supplement_2):S162-S165.

18. Fang FC. Perspectives series: host/pathogen interactions. Mechanisms of nitric oxide-related antimicrobial activity. *The Journal of clinical investigation.* 1997;99(12):2818-2825.

19. Wo Y, Brisbois EJ, Bartlett RH, Meyerhoff ME. Recent advances in thromboresistant and antimicrobial polymers for biomedical applications: just say yes to nitric oxide (NO). *Biomaterials science.* 2016;4(8):1161-1183.

20. Mathews WR, Kerr SW. Biological activity of S-nitrosothiols: the role of nitric oxide. *Journal of Pharmacology and Experimental Therapeutics.* 1993;267(3):1529-1537.

21. Goudie MJ, Brisbois EJ, Pant J, Thompson A, Potkay JA, Handa H. Characterization of an S-nitroso-N-acetylpenicillamine–based nitric oxide releasing polymer from a translational perspective. *International Journal of Polymeric Materials and Polymeric Biomaterials.* 2016;65(15):769-778.

22. Vaughn MW, Kuo L, Liao JC. Estimation of nitric oxide production and reactionrates in tissue by use of a mathematical model. *American Journal of Physiology-Heart and Circulatory Physiology.* 1998;274(6):H2163-H2176.

23. Singha P, Pant J, Goudie MJ, Workman CD, Handa H. Enhanced antibacterial efficacy of nitric oxide releasing thermoplastic polyurethanes with antifouling hydrophilic topcoats. *Biomaterials Science.* 2017.

24. Moynihan HA, Roberts SM. Preparation of some novel S-nitroso compounds as potential slow-release agents of nitric oxide in vivo. *Journal of the Chemical Society, Perkin Transactions 1.* 1994(7):797-805.

25. Liu J, Hsieh YZ, Wiesler D, Novotny M. Design of 3-(4-carboxybenzoyl)-2-quinolinecarboxaldehyde as a reagent for ultrasensitive determination of primary amines by capillary electrophoresis using laser fluorescence detection. *Analytical chemistry.* 1991;63(5):408-412.

26. Ellman GL. Tissue sulfhydryl groups. *Archives of biochemistry and biophysics.* 1959;82(1):70-77.

27. El-Newehy MH, Alamri A, Al-Deyab SS. Optimization of amine-terminated polyacrylonitrile synthesis and characterization. *Arabian Journal of Chemistry.* 2014;7(2):235-241.

28. Saino E, Focarete ML, Gualandi C, et al. Effect of electrospun fiber diameter and alignment on macrophage activation and secretion of proinflammatory cytokines and chemokines. *Biomacromolecules.* 2011;12(5):1900-1911.

29. Badami AS, Kreke MR, Thompson MS, Riffle JS, Goldstein AS. Effect of fiber diameter on spreading, proliferation, and differentiation of osteoblastic cells on electrospun poly (lactic acid) substrates. *Biomaterials.* 2006;27(4):596-606.

30. Bashur CA, Dahlgren LA, Goldstein AS. Effect of fiber diameter and orientation on fibroblast morphology and proliferation on electrospun poly (D, L-lactic-co-glycolic acid) meshes. *Biomaterials.* 2006;27(33):5681-5688.

31. Webb K, Hlady V, Tresco PA. Relative importance of surface wettability and charged functional groups on NIH 3T3 fibroblast attachment, spreading, and cytoskeletal organization. *Journal of Biomedical Materials Research: An Official Journal of The Society for Biomaterials, The Japanese Society for Biomaterials, and the Australian Society for Biomaterials.* 1998;41(3):422-430.

32. Williams DLH. The chemistry of S-nitrosothiols. *Accounts of chemical research.* 1999;32(10):869-876.

33. Coneski PN, Nash JA, Schoenfisch MH. Nitric oxide-releasing electrospun polymer microfibers. *ACS applied materials & interfaces.* 2011;3(2):426-432.

34. Lowe A, Bills J, Verma R, Lavery L, Davis K, Balkus Jr K. Electrospun nitric oxide releasing bandage with enhanced wound healing. *Acta biomaterialia.* 2015;13:121-130.

35. Hopkins SP, Pant J, Goudie MJ, Schmiedt C, Handa H. Achieving long-term biocompatible silicone via covalently immobilized S-nitroso-N-acetylpenicillamine (SNAP) that exhibits 4 months of sustained nitric oxide release. *ACS applied materials & interfaces.* 2018.

36. Vetrik M, Parizek M, Hadraba D, et al. Porous Heat-Treated Polyacrylonitrile Scaffolds for Bone Tissue Engineering. *ACS Appl. Mater. Interfaces.* 2018;10(10):8496-8506.

37. Ziche M, Morbidelli L, Masini E, et al. Nitric oxide mediates angiogenesis in vivo and endothelial cell growth and migration in vitro promoted by substance P. *The Journal of clinical investigation.* 1994;94(5):2036-2044.

38. Garg UC, Hassid A. Nitric oxide-generating vasodilators and 8-bromo-cyclic guanosine monophosphate inhibit mitogenesis and proliferation of cultured rat vascular smooth muscle cells. *The Journal of clinical investigation.* 1989;83(5):1774-1777.

39. Luo J-d, Chen AF. Nitric oxide: a newly discovered function on wound healing. *Acta Pharmacol. Sin.* 2005;26(3):259.

40. Shekhter AB, Serezhenkov VA, Rudenko TG, Pekshev AV, Vanin AF. Beneficial effect of gaseous nitric oxide on the healing of skin wounds. *Nitric oxide.* 2005;12(4):210-219.

41. Han G, Nguyen LN, Macherla C, et al. Nitric oxide–releasing nanoparticles accelerate wound healing by promoting fibroblast migration and collagen deposition. *The American journal of pathology.* 2012;180(4):1465-1473.

42. Schäffer MR, Tantry U, Gross SS, Wasserkrug HL, Barbul A. Nitric oxide regulates wound healing. *J. Surg. Res.* 1996;63(1):237-240.

43. Tsibouklis J, Stone M, Thorpe A, et al. Preventing bacterial adhesion onto surfaces: the low-surface-energy approach. *Biomaterials.* 1999;20(13):1229-1235.

44. Privett BJ, Broadnax AD, Bauman SJ, Riccio DA, Schoenfisch MH. Examination of bacterial resistance to exogenous nitric oxide. *Nitric Oxide.* 2012;26(3):169-173.

CHAPTER 4

CONCLUSIONS AND FUTURE WORK

4.1 CONCLUSIONS

This research demonstrates two successful methods for enhancement of NO release and duration from polymeric materials. Chapter 2 is the first report of the combination of zinc oxide nanoparticles and an RNSO donor within a single material. By incorporating the zinc catalyst into the topcoat of a SNAP-CarboSil®, we were able to extend the NO release by 7 days and maintain physiologically relevant levels. The films containing no catalyst had NO exhausted after 24 hours when left in physiological conditions. By using zinc as the metal catalyst, the NO-releasing films had an additional method for antimicrobial action, as metal ions have been proven highly successful bactericidal agents. The combination of Zinc oxide and SNAP was able to reduce viable bacteria on the film surface by 99% compared to the control, whereas only zinc and only SNAP were able to reduce adhesion by 78% and 87%, respectively. Overall, the preliminary studies of our novel material showed no cytotoxic effects and excellent retention of our NO donor.

Chapter 3 described a unique approach to the development of NO-releasing fibers. The direct attachment of a NO donor to a polymer substrate can prolong NO release. Electrospun polymeric fibers are useful materials for wound healing applications, specifically wound dressings. Previous studies of NO-releasing polymeric fibers reported NO release exhausted at only 4 hours. To enhance this release, we covalently attached an

RNSO molecule to polyacrylonitrile (PAN) prior to electrospinning to eliminated leaching of the NO donor. Once spun, our fibers had NO flux of 0.70 x 10^{-10} mol min^{-1} cm^{-2} at 6 hours and 0.38 x 10^{-10} mol min^{-1} cm^{-2} at 24 hours. The SNAP-PAN scaffold was able to provide an adequate environment to support fibroblast migration and proliferation due to its hydrophilic nature. The NO component provided the fibers with defense against *S. aureus*, with a 2-log reduction of viable bacteria compared to control PAN fibers. SNAP-PAN fibers show excellent potential for wound healing application where new tissue growth is desired and infection prevention is needed.

4.2 FUTURE WORK

Both studies provide the initial development of two innovative NO-releasing materials for medical applications. Further characterization of these materials will be needed before moving to clinical application. A mouse wound model can be used to evaluate the *in vivo* effectiveness of SNAP-PAN fibers on wound closure and healing. Expanding to *in vivo* studies will allow for a deeper understanding how other components of the human body, such as inflammation factors and immune cells, may impact the materials effect on wound healing. Future work for the zinc topcoat study will be the expansion of the topcoat to various medical grade polymers, to allow for the multi-antimicrobial system to be used in a variety of clinical application. In summary, this work is a step towards reducing HAIs, while retaining the ability to continue the use of lifesaving medical devices.

APPENDIX A

SUPPLEMENTAL INFORMATION FOR CHAPTER 2

Complementary Table of values from **Figure 2.6**:

Sample	% Relative Cell Viability
CarboSil	100 ± 3.11
ZnO	95.88 ± 11.36
SNAP	99.98 ± 10.27
SNAP-ZnO	91.21 ± 5.31

Reaction Theory for Zinc-Catalyzed NO generation:

Typical NO Generation $RSNO \xrightarrow[\text{Heat, Light, Moisture}]{} NO\cdot + RS\cdot \longrightarrow RSSR$

$RSNO \xrightarrow{Zn^{2+}} NO^{+} + RS^{-}{}_{(---Zn^{2+})}$

Side Reaction $(RSH + NO\cdot \longrightarrow RSNO)$

$RSNO \xrightarrow{NO^{+}} 2NO\cdot + RS\cdot$

APPENDIX B

SUPPLEMENTAL INFORMATION FOR CHAPTER 3

Schematic for Electrospinning Set Up: